BENEFICIATION AND TREATMENT OF BRINE FROM TREATMENT OF MINING EFFLUENT

R. Weideman, N. Chiwaye, K du Preez

WATER RESEARCH COMMISSION

TT 947/24

BENEFICIATION AND TREATMENT OF BRINE FROM TREATMENT OF MINING EFFLUENT

Final Report

Report
to the Water Research Commission

by

R. Weideman, N. Chiwaye, K du Preez
Biometallurgy Division, Mintek

WRC report no. TT 947/24
ISBN 978-0-6392-0676-9

January 2025

Obtainable from
Water Research Commission
Private Bag X03
Gezina, 0031

hendrickm@wrc.org.za or download from www.wrc.org.za

This is the final report of WRC project no. C2019/2020-00100.

EXECUTIVE SUMMARY

BACKGROUND

South Africa's mining industry has played a significant role in the nation's economic development. However, the closure of coal mines in recent decades has led to the discharge of mine-influenced water (MIW) that requires management post-mine closure. Currently, the mines treat the MIW by neutralisation and discharge to rivers or through centralised reverse osmosis plants to produce potable water for local municipalities. The reverse osmosis membrane process generates substantial volumes of brine waste, which poses a significant challenge in terms of disposal or further treatment.

Developing cost-effective and environmentally sound solutions for brine disposal or recovery of valuable components from the brines remains a critical area of research and development.

Mineral carbonation offers a promising alternative by reacting CO_2 with Mg- and Ca-containing liquid mine wastes to produce stable carbonates. This approach addresses both CO_2 sequestration and MIW brine treatment, potentially yielding valuable products while mitigating environmental and legal liabilities. Research gaps remain in optimising carbonation processes for cost-effectiveness, resource recovery, and large-scale implementation, highlighting the need for innovative solutions in AMD brine management and carbon capture.

AIMS

The main aim of this project was to use mineral carbonation as a low-cost method to beneficiate and remediate Mg- and Ca-containing liquid mine wastes (brines) in a continuous process to produce chemical products (*i.e.*, carbonates) for re-use in the mining industry and carbon sequestration.

The specific objectives included the following:

1. beneficiating liquid mine waste by producing valuable products (carbonate precipitates),
2. piloting the process on a continuous basis under optimised conditions,
3. producing a magnesium oxide product prototype through calcination of the nesquehonite precipitate,
4. developing a process model to assess process performance using alternative brine solutions, and
5. assessing the financial feasibility through desk-top analysis.

SCOPE AND LIMITATIONS

This project entailed piloting the mineral carbonation process continuously in a lab-scale pilot test work, while treating an industrial mine waste (brine) sample. Laboratory optimisation of the process was undertaken, and the optimum conditions were implemented during the pilot-scale investigations.

The results from previously conducted optimisation work demonstrated that it was possible to produce two separate products of relatively high purity from an industrial brine solution using an improved, “two-step” mineral carbonation process. It is this new, improved “two-step” process that was piloted on a continuous basis for the WRC project C2019/2020-00100.

METHOD

The first part of the investigation focused on the laboratory-scale optimisation of two main process parameters: the CO_2 gas flow rate and hydraulic residence time (HRT). The experimental approach aimed to reduce CO_2

gas flow rates while monitoring the removal of calcium and magnesium from the solution. This step was necessary as excessive CO_2 supply led to increased NaOH consumption to maintain the pH at 9.5. CO_2 dissolves and forms bicarbonate ions that lower the pH of the solution. By minimising the CO_2 flow rate, the goal was to achieve maximum sequestration efficiency while reducing NaOH consumption, resulting in operational cost savings. Additionally, HRT optimisation ensured maximal removal of calcium and magnesium, guaranteeing the production of purer products. Tests at varying flow rates facilitated the determination of the optimal values for enhanced efficiency and cost-effectiveness.

To establish a baseline understanding of the process at pilot-scale, the operability of the two-stage continuous pilot plant carbonation system was demonstrated using an industrial brine sample. Over five hours, 100 ℓ of effluent passed through the reactor, and the final product was collected as a solid. For the second stage, the filtrate from the first stage was collected and passed through the reactor under the same conditions, and the final product was collected as a solid.

Following the baseline pilot runs, additional pilot runs were conducted to assess the performance of the optimised pilot plant conditions. These runs aimed to validate the laboratory-scale optimisations in a pilot-scale setting, ensuring the proposed adjustments effectively enhanced the process's efficiency and cost-effectiveness. The products formed during these pilot runs were characterised using X-ray diffraction to identify, confirm and quantify the purities of the products formed during each stage of the process.

The product formed during the second stage of the process, which consisted mainly of the target mineral nesquehonite, was calcined to determine the final product purity for the assessment of process feasibility.

A mathematical model was developed to describe the carbonation process, focusing on the rates of CO_2 dissolution and carbonate precipitation. The model uses differential equations to track the concentrations of CO_2, Ca^{2+}, and Mg^{2+} over time, considering factors such as initial concentrations, flow rates, and reactor volume.

The feasibility of the process was investigated by conducting a techno-economic assessment under various setups and conditions. The process model was developed using results from optimised pilot operations. To evaluate its feasibility at scale, the model was scaled based on the estimated daily brine production of the eMalahleni Water Reclamation Plant (EWRP), which treats between 50 Mℓ and 60 Mℓ of AMD per day. Assuming a 60 % water recovery rate, the plant produces approximately 20 Mℓ of brine daily. This scale was chosen to ensure a realistic application of the process.

To evaluate the feasibility of the process, three process flow sheets were considered:

1. **Single-stage process:** This approach aims to generate a calcium and magnesium carbonate complex product of relatively lower value, streamlining the operation into a single stage to potentially halve the capital costs.
2. **Two-stage process:** In this setup, the first stage yields a magnesium and calcium carbonate complex product, while the subsequent stage focuses on producing a high-purity magnesium carbonate product.
3. **Calcination step addition:** This process includes a calcination step after the two-stage process to produce MgO as a final product.

Further investigation was conducted to determine the viability of the process under varying brine magnesium and calcium concentrations. The impact of magnesium removal efficiency in the second stage on overall process feasibility was also assessed. Additionally, the effect of CO_2 price reduction on the feasibility of the process was evaluated.

RESULTS AND DISCUSSION

Laboratory scale optimisation

The optimisation of the two key process parameters, namely CO_2 gas flow rate and HRT, was successfully accomplished through systematic experimentation and analysis at laboratory scale. The findings of this study are summarised as follows:

Co_2 gas flow rate optimisation:

- Stage 1: An inflection point was observed at a CO_2 feed rate of 2.13 ℓ CO_2/ ℓ brine/hour, beyond which calcium concentration in solution began to increase, indicating suboptimal removal.
- Stage 2: A similar inflection point was identified at 2.84 ℓ CO_2/ℓ brine/hour, where magnesium concentration started rising due to inadequate CO_2 supply.

HRT optimisation:

- Stage 1: Maximum calcium removal was calculated at an HRT of 1.54 hours.
- Stage 2: Maximum magnesium removal was calculated at an HRT of 1.52 hours.

Baseline pilot runs: establishing process norms

Both raw and dosed brine feedstocks exhibited rapid calcium removal, reaching maximum removal percentages of 100.00 % and 96.63 %, respectively. This consistency demonstrates promising repeatability. In contrast, magnesium removal showed variability, with both feedstocks achieving around 50 % maximum removal. The raw brine failed to sustain the removal rates achieved by the dosed brine, highlighting the complex nature of brine treatment due to factors like competing ions and carbonate precipitation dynamics.

The dosed brine had a significantly higher product production rate (113.77 g/h) compared to the raw brine (41.40 g/h), indicating the substantial influence of chemical composition on CO_2 sequestration efficacy. Despite similar magnesium removal percentages, the dosed brine's higher magnesium concentrations led to significantly increased removal and production rates. Elevated calcium removal in the dosed brine, attributed to higher sulphate concentrations, supports the need for magnesium concentrations above 1000 mg/ℓ to maximise CO_2 sequestration rates.

Calcium levels remained low in Stage 2 due to high recovery rates in Stage 1, so removal percentages were not provided. Magnesium removal was slightly higher for the raw brine (34.25 %) compared to the dosed brine (28.17 %). The decline in the dosed brine's removal rate was likely due to increased sulphate concentrations, impacting magnesium removal efficacy

Seeding with nesquehonite improved magnesium removal significantly, with the seeded run achieving around 29 % removal compared to 11 % in the unseeded run. This enhancement is attributed to the additional nucleation sites provided by the seed crystals, which facilitated faster precipitation kinetics.

Elevated sulphate concentrations negatively affected magnesium removal, decreasing from 57 % at 5.2 g/ℓ sulphate to 17 % at 16 g/ℓ sulphate. Calcium removal was less affected but still decreased from 90 % to 78 % under the same conditions, highlighting sulphate’s more pronounced inhibitory effect on magnesium carbonation.

Steady state operation of optimised pilot runs

The steady-state optimised pilot operation for mineral carbonation of brine was conducted in two stages, focusing on the removal of calcium and magnesium. In Stage 1, the process achieved peak calcium removal of between 81 % and 88 % and magnesium removal of approximately 50 %. However, high sulphate concentrations in the feed brine (34 g/ℓ to 36 g/ℓ) negatively impacted removal efficiencies compared to baseline runs. The primary products identified through XRD analysis were monohydrocalcite and nesquehonite, with precipitate production rates of 77 g/ℓ and 82 g/h.

Stage 2 of the process, designed to focus on magnesium removal, demonstrated peak removal efficiencies of 24 % - 26 % within the first 2-3 hours of operation, stabilising around 20 % thereafter. Seeding was employed to enhance precipitation, resulting in improved performance compared to baseline runs. The primary product of Stage 2 was nesquehonite, comprising 89.0 % - 92.7 % of the precipitate as determined by XRD analysis.

A prototype magnesium oxide product was successfully produced through calcination of the Stage 2 precipitates at 850 °C. The resulting product contained 81.8 % - 88.2 % periclase (MgO), demonstrating the potential for high-purity MgO production from the carbonation process.

Despite the successful removal of calcium and magnesium, the process faced significant challenges. The continuous addition of NaOH for pH control led to a substantial increase in sodium concentrations in the treated water, reaching 38 800 mg/ ℓ. This high sodium content, along with residual magnesium (589 mg/ ℓ), presents obstacles for water reuse or environmental discharge. The study highlights the potential of mineral carbonation for brine treatment while underscoring the need for further optimisation to address challenges related to high sulphate concentrations and sodium accumulation.

PREDICTIVE MODEL

The model parameters were fitted using experimental data from Stage 1 and Stage 2 runs. Reaction rate constants were determined:

- k1 (CO_2 dissolution): 9.99×10^{-3} s^{-1}
- k5 ($CaCO_3$ precipitation): 8.08×10^{-4} M^{-1} s^{-1}
- k6 ($MgCO_3$ precipitation): 1.65×10^{-4} M^{-1} s^{-1}

Comparison of modelled and experimental data showed good agreement for final concentrations, with errors of 21 % for Mg and 15 % for Ca in Stage 1, and 17 % for Mg in Stage 2. However, the model overestimated initial removal rates, particularly for magnesium, suggesting the presence of unaccounted inhibitory effects, possibly related to crystalline growth.

Despite some limitations, the model provides a robust understanding of the carbonation process and was used in the techno-economic assessments to determine optimal conditions for financial viability when treating brines of varying concentrations.

Techno economic feasibility investigation

The economic feasibility analysis highlighted the significant challenges associated with the proposed processes. It was determined that the process must function as a two-stage system, producing carbonates as products. This is due to the low-value mixed $CaMgCO_3$ product produced in a single-stage process and the low market value of MgO compared to $MgCO_3$, which is produced in a three-stage process where the CO_2 sequestered is re-released into the environment.

The primary limiting factors for the financial feasibility of the two-stage process are:

1. The low availability of adequate mineral concentrations in the feed water, and
2. The low recovery rates of magnesium achieved in the second stage of the process.

The major driver of operational costs is NaOH, constituting at least 80 % of the operational expenses.

CONCLUSIONS

Several key conclusions can be drawn from the piloting of the two-stage mineral carbonation process for CO2 sequestration and valuable product recovery from brine. The study demonstrated the technical feasibility of the process, achieving high calcium removal rates and improved magnesium removal through optimised seeding strategies in the second stage. The production of high-purity nesquehonite (89 % - 93 %) in Stage 2

and subsequent calcination to high-purity MgO (81.8 % - 88.2 % periclase) highlights the potential for generating valuable products.

The economic viability of the process is heavily dependent on the mineral content of the feed brine. The techno-economic assessment indicated that the process was financially viable when treating high mineral content brines, with potential revenue exceeding 190 % of operational expenses and an internal rate of return of 27.3 %. Additional recovery stages may improve gross revenue; they also introduce higher costs that outweigh the benefits in terms of the rate of return. However, the process faces significant economic challenges due to high operational costs, predominantly driven by NaOH consumption for pH control, which accounts for approximately 84 % of total operational expenses.

From an environmental perspective, the process effectively sequesters CO_2 but produces high-sodium-treated water, posing challenges for disposal or reuse. The developed predictive model demonstrates good alignment with experimental data, particularly in estimating final concentrations, providing a valuable tool for process optimisation and scale-up considerations. However, its limitations in capturing initial kinetics suggest complex inhibitory effects that warrant further study. Additionally, elevated sulphate concentrations negatively impact magnesium removal efficiency, presenting a significant technical hurdle that requires further investigation and mitigation strategies.

RECOMMENDATIONS

Firstly, future research should focus on optimising the process for high mineral content brines, such as those from seawater desalination, to maximise economic potential. Concurrently, investigation into alternative pH control methods, particularly the use of magnesium hydroxide, could significantly reduce operational costs due to the recovery of the neutralising agent in the product, without adding sodium to the brine, which is already difficult to remediate.

Further process optimisation efforts should target improved magnesium removal rates and consistency, with a specific emphasis on developing strategies to mitigate the adverse effects of high sulphate concentrations. Exploration of low-cost or captured CO_2 sources could further enhance the economic viability of the process and assess the impacts of pollutants on the purity of the produced products. Additionally, conducting larger-scale pilot studies using high mineral content brines is crucial to validate economic projections and process performance at an industrial scale.

From an environmental perspective, a comprehensive lifecycle assessment is recommended to quantify the net environmental benefits, including CO_2 sequestration potential and the implications of treated water management. This assessment should inform the development of integrated solutions for brine treatment and CO_2 sequestration within broader water management and climate mitigation strategies.

ACKNOWLEDGEMENTS

The project team wishes to thank the following people for their contributions to the project.

Reference Group	Affiliation
John Ngoni Zvimba (Chairperson)	Water Research Commission
Bennie Mokgonyana (Co-ordinator)	Water Research Commission
Jenny Broadhurst	University of Cape Town
Dave Dew	University of Exeter
Sello Ndlovu	University of the Witwatersrand
Bashan Govender	Department of Water and Sanitation
Sharon Mogomotsi	Department of Environment Forestry and Fisheries
Hlanganani Tutu	University of the Witwatersrand
JP Maree	University of Limpopo
Molefe Morokane	Department of Mineral Resources and Energy
Mintek Team	
	Reinhardt Weideman
	Natsayi Chiwaye
	Ryan Merckel
	Kerri du Preez
	Dylan Naidoo
	Mahlatse Tema
	Petrus Basson
	Tamsyn Grewar
	Donald Shai

CONTENTS

LIST OF FIGURES

LIST OF TABLES

ACRONYMS & ABBREVIATIONS

WRC	Water Research Commission
CO_2	Carbon dioxide
AMD	Acid mine drainage
EWRP	eMalahleni Water Reclamation Plant
NQ	Nesquehonite
MC	Mineral carbonation
MgO	Magnesium oxide
GHG	Green-house-gas
MHC	Monohydrocalcite
CSTR	Continuously stirred tank reactors
USD	United States Dollar
MT	Metric tonne
CAGR	Compounded annual growth rate
$CaCO_3$	Calcium carbonate
$MgCO_3$	Magnesium carbonate

GLOSSARY

Calcination	A thermal process applied to solid chemical compounds, such as mixed carbonate ores, where the material is heated to elevated temperatures without reaching its melting point. This occurs under a controlled oxygen supply (typically with limited gaseous oxygen present in the air) to facilitate the removal of impurities, volatile components, or to induce thermal decomposition.
Carbonation	A chemical process involving the reaction of carbon dioxide to produce carbonates, bicarbonates, or carbonic acid. In some contexts, the term may also refer to carboxylation, which is the formation of carboxylic acids.
CO_2 mineralisation	A technique used to capture and convert carbon dioxide into stable carbonated minerals, serving as a method for long-term carbon storage
CO_2 sequestration	the process of capturing carbon dioxide from the atmosphere and storing it to reduce its concentration. This approach aims to mitigate climate change by lowering atmospheric CO_2 levels
Techno-economic analysis	An evaluation method that examines the economic feasibility of an industrial process, product, or service. It often involves the use of modelling software to calculate capital costs, operational expenses, and potential revenues based on both technical and financial inputs.

CHAPTER 1: BACKGROUND

1.1 INTRODUCTION

South Africa's mining industry has played a significant role in the nation's economic development. However, the closure of coal mines in recent decades has led to the discharge of mine-influenced water (MIW) that requires management post-mine closure. Uncontrolled discharge can contaminate freshwater resources, resulting in long-lasting ecological damage to waterways, biodiversity loss, and adverse health impacts on communities reliant on these resources (Akcil & Koldas, 2006; Naidoo, 2017; Cunha *et al*., 2019).

Currently, the mines treat MIW by neutralisation on site and discharge to rivers or through centralised reverse osmosis plants to produce potable water for local municipalities. The reverse osmosis membrane process employed for MIW treatment generates substantial volumes of brine waste, which poses a significant challenge in terms of disposal or further treatment (Bai *et al*., 2013; Dhir, 2018). These brines typically contain high concentrations of dissolved salts, such as sulphate, chloride, and calcium derivatives which are concentrated during the reverse osmosis (RO) and other membrane filtration processes (Simate & Ndlovu, 2014).

These brines have salinity levels ranging from 65 000 mg/ ℓ to 85 000 mg/ℓ, three times the salinity of seawater (Abdul-Wahab & Al-Weshahi, 2009), and they cannot be directly discharged to the environment. Improper disposal can lead to soil and groundwater contamination, adversely impacting ecosystems and posing risks to human health (Simate & Ndlovu, 2014). Furthermore, the large volumes of brines produced during the treatment of AMD necessitate costly disposal or treatment methods, such as evaporation ponds, deep well injection, or advanced treatment processes like crystallisation or thermal treatment. These additional steps contribute significantly to the overall operational costs. Desalination processes face similar significant challenges in managing brine by-products (Lattemann & Höpner, 2008; Miri & Chouikhi, 2005).

Addressing the challenge of brine management is crucial for the effective and sustainable implementation of membrane filtration technologies for AMD treatment. Developing cost-effective and environmentally sound solutions for brine disposal or recovery of valuable components from the brines remains a critical area of research and development.

1.1.1 Treatment of brines

Disposal methods for brine include deep well injection, land application, evaporation ponds, discharge into sewer systems, direct release into surface waters, use in aquaculture, and beneficial reuse through salt recovery and harvesting systems (Table 1-1, Mezher *et al*., 2010).

Table 1-1. Disposal methods used by some countries (Mezher *et al*., 2010 and references therein)

Country	Disposal method
Qatar	Land application and evaporation ponds
Jordan	Land application and evaporation ponds
Oman	Land application and evaporation ponds
Kingdom of Saudi Arabia	Evaporation ponds
Australia	Evaporation ponds
Kuwait	Evaporation ponds
China	Land application
United Arab Emirates Surface water	Surface water

Country	Disposal method
Spain	Surface water
Japan	Surface water
Algeria	Surface water
United Kingdom	Sewer system blending and land application
United States of America	United States of America Surface water, sewer system blending, land application, evaporation ponds, and deep well injection (in increasing order of percentage use)

Brine waste management methods have been categorised into four types (Giwa *et al*., 2017) namely:

1. minimisation approaches such as further membrane RO and chemical pre-treatment steps,
2. thermal based minimisation strategies which include evaporators, driers and distillation membranes,
3. direct disposal approaches, and
4. possible recovery of salts through crystallisation and evaporative cooling.

Wetlands rejuvenation by use of brine has also been studied, and possible agriculture irrigation has been assessed. These methods, however, do have some notable challenges; for example, the common use of evaporation ponds for minimising brine produces a hyper saline brine waste. Further, brine dams present a risk of the brine percolating and leaking into the soil and evaporation ponds require a sizable land footprint, that can be up to 4 km^2 to handle the high volumes produced (GreenCape 2019). Fouling of equipment is the biggest challenge that heat treatment strategies for treating brine face (Giiwa *et al.,* 2017). Generally, brine disposal in landfills and sea is also costly (GreenCape 2019). Alternative methods for the disposal of brine continue to be an important field of study for countries with access to the sea that consider desalination through RO for potable water production. Cheaper and more environmentally friendly methods of brine management would also make RO treatment of MIW economical and lead to wider-scale adoption. Both desalination due to water scarcity and treatment of MIW are becoming increasingly applicable in South Africa.

1.1.2 Greenhouse Gases

South Africa is ranked as the 15th highest greenhouse gas (GHG) emitting country globally (IEA, 2023) and energy generation from coal is a chief contributor to the total carbon emissions in the country at 83 %. South Africa will soon be required to reduce its total emissions to comply with the Paris Agreement. CO_2 is the most important greenhouse gas due to the enormous amounts produced from anthropogenic activities and it continues to increase in concentration in the atmosphere.

The Carbon Tax Act was signed into law in South Africa in May 2019 and came into effect on 1 June 2019 (eNCA, 2019). The implications of carbon tax on industry as a whole have highlighted the need for new technologies to be developed rapidly to mitigate potential carbon costs. Carbon capture and utilisation seeks to make use of the CO_2 captured as a raw material to produce valuable products that generate revenue (IEA, 2024).

These challenges could yield potential opportunities for development of technologies to minimise water use, emissions and environmental liabilities for mines and industry. Various methods of capture are at different stages of technology development (Wu *et al*., 2024) and can be extremely costly. One process that has the potential to address mine water remediation as well as to off-set costs through waste beneficiation and reduce carbon tax liabilities, is carbonation. This process involves bubbling CO_2 through an alkaline solution rich in Ca/Mg/Fe ions which results in carbonate formation, sustainably trapping CO_2. For this reason, this process is

often used as a carbon sequestration method, although in this project, it will be utilised primarily as a method for beneficiating suitable liquid wastes.

Power generation and mining industries are large carbon point emitters and can be producers of RO brine from MIW treatment. Hypothetically, this aspect makes them good candidates for carbonation since both raw materials (Mg-Ca waste effluent materials and CO_2) are present in the same vicinity creating an opportunity to reduce the cost of transporting CO_2 to points of storage. As a result, there is an opportunity to realise benefits through carbon emission reduction and offset carbon-tax while adding value to waste and simultaneously reducing environmental liabilities from mine water discharge. The process is also useful for regions with limited CO_2 storage sites.

1.1.3 Mineralisation Using CO_2

Carbonation is the reaction of CO_2 gas with alkaline earth metals bearing silicate/hydroxide minerals to form carbonate minerals which are stable and inert, sustainably trapping CO_2. It is a natural process that usually occurs over glacial timeframes (such as in the formation of dolomites) but can be accelerated through chemical and physical means (Olajire, 2013; Nyambura *et al*., 2011). There are many applications for CO_2 sequestration, although the most common applications focus on the carbonation of waste mine tailings and other solid sources of silicate minerals containing calcium and magnesium.

Current methods for carbonation focus on CO_2 sequestration as the primary purpose and include adsorption by physical and chemical wet scrubbing, adsorption by solids using high pressures and temperatures, cryogenic distillation and mineral carbonation (Nyambura *et al*., 2011). Mineral carbonation is an attractive method for carbon sequestration as it results in permanent storage of CO_2 as environmentally benign mineral carbonates. It can also be used to produce products of value for reuse in a variety of activities (Olajire, 2013, Nyambura *et al*., 2011).

A process that uses carbonation to form carbonate minerals is known as the “Indirect pH-swing” method. The initial (and rate-limiting) step includes the leaching of Ca-Mg-Fe cations from silicates using acids or other harsh chemicals. The pH is then increased to between 9 and 10 followed by carbonation, which is essentially the bubbling of CO_2 gas through the solution. This is usually undertaken at high temperatures and pressures to form carbonate precipitates (*i.e*., inactive minerals such as dolomite, siderite, magnesite, *etc*.) (Naidoo, 2013).

In general, mineral carbonation is very energy intensive as it typically requires extreme operating conditions and the handling of large amounts of chemical reagents during the initial extraction step. To date, this has been the primary barrier to entry for this particular technology, and the research focus has since shifted to speeding up the dissolution of the target minerals or using alkaline solid wastes as the Mg-Ca resources (Siriruang *et al*., 2017; Ji *et al*., 2017; Dananjayan *et al*., 2016). The optimal temperature and pressure conditions are also being investigated but require new innovations to reduce energy requirements to realise an economically viable process (Naidoo, 2013). Nevertheless, the extraction kinetics and costs remain the primary obstacle for large-scale application (Fagerlund *et al*., 2010).

Another avenue of research being explored is the use of liquid waste resources for carbonation in order to bypass the costly and rate-limiting extraction step. Bang *et al*. (2017) investigated the potential of using a brine sample from seawater desalination plants for CO_2 mineralisation. Similarly, Galvez-Martos *et al*. (2018) investigated the production of nesquehonite (NQ) using a synthetic brine solution. They found that the presence of calcium in the brine interfered with the purity of the nesquehonite, hence the authors proposed a multi-stage precipitation process to improve the purity of the end-product. Although the use of brines as a potential source of calcium and magnesium is promising due to the elimination of the extraction step, the authors highlighted that the cost associated with bringing these waters to neutral pH is a significant disadvantage. Galvez-Martos and co-authors (2018) had targeted the construction industry for use of the nesquehonite, and waste remediation was not a part of their focus.

1.1.4 Nesquehonite as a Value Product

The mining industry is the potential end user for nesquehonite formed in this process as MgO is used extensively during metal recovery in hydrometallurgical processes, and the industry is facing liabilities associated with treatment of mine water streams discharged from their sites. Nesquehonite can act as a preferential MgO precursor due to its hydrated nature, and therefore the value of nesquehonite is closely linked to that of MgO. Hydrated nesquehonite allows for lower calcination temperatures and faster dehydration and decarbonation reaction rates during the thermal preparation of MgO, which reduces the costs of MgO production, benefiting the end-user (Ren *et al*., 2014).

1.1.5 Improved Two Step Process for Formation of Mg Products

The focus for this project has been to develop the process for beneficiation of MIW brines, for operation under ambient conditions of pressure and temperature to lower operational and capital equipment costs. Prior work conducted in the Biometallurgy Division of Mintek focused on optimising the production of a $MgCO_3$ derivative, namely nesquehonite (NQ) at bench-scale. The carbonate was produced from synthetic Mg-rich solutions using mineral carbonation in a one-step process.

Mintek filed a New Discovery document (17/0/447) and a NIPMO (NIPMO CR2018-033). This discovery relates to the process for the production of a high value solid $MgCO_3$ (nesquehonite) product by carbonation (with CO_2) of liquid solutions containing Mg ions (such as but not limited to acid mine-drainage, hydrometallurgical leachates, gypsiferous mine-water, *etc*.) under alkaline conditions. The $MgCO_3$ product can then ultimately be used as a feed source for the production of the even higher value product MgO. The process essentially consists of two primary steps:

Step 1: Clean up

As stated above, the feed source for $MgCO_3$ production is liquid solutions containing Mg ions which most likely will also contain other elements. A precipitation clean-up protocol is initiated by the addition of an alkaline additive (such as but not limited to NaOH, limestone or other alkaline materials/wastes). This step targets precipitation of Ca and other salt compounds to leave a Mg-rich water for product formation in Step 2.

Step 2: $MgCO_3$ formation

Once the required pH has been reached and other contaminants removed, the alkaline Mg-containing solution is carbonated by a CO_2 gas source (such as but not limited to a commercially pure CO_2 gas stream, a CO_2 waste-stream such as but not limited to those emitted from coal-fired power stations or the CO_2 emitted during MgO production from $MgCO_3$, which may also be captured and recycled in this process) thereby forming a high value $MgCO_3$ solid product.

The $MgCO_3$ product is then calcined to form MgO.

The mineral carbonation process investigated in this study can be represented by Equations 1 to 8 (Mitchell, *et al*., 2010).

$$CO_2(g) \rightleftharpoons CO_2(aq) \quad [1]$$

$$CO_2(aq) + H_2O(l) \rightleftharpoons H_2CO_3(aq) \quad [2]$$

$$H_2CO_3(aq) \rightleftharpoons H^+(aq) + HCO_3^-(aq) \quad [3]$$

$$HCO_3^-(aq) \rightleftharpoons H^+(aq) + CO_3^{2-}(aq) \quad [4]$$

$$Ca^{2+}(aq) + CO_3^{2-}(aq) \rightleftharpoons CaCO_3(s)\downarrow \quad [5]$$

$$Mg^{2+}(aq) + CO_3^{2-}(aq) \rightleftharpoons MgCO_3 \cdot 3H_2O(s)\downarrow \quad [6]$$

$$NaOH(aq) \rightleftharpoons Na^+(aq) + OH^-(aq) \quad [7]$$

$$H^+(aq) + OH^-(aq) \rightleftharpoons H_2O(l) \quad [8]$$

In South Africa, the feasibility of alternative strategies for brine management and CO_2 capture remains underexplored. Key questions include how to reduce costs associated with these processes and whether brine can be utilised to recover valuable products. Current research predominantly focuses on seawater-based carbon capture, yielding products like $MgCO_3$ and $CaCO_3$. Expanding this focus to include AMD brine could open new opportunities for sustainable brine management and contribute to the development of cost-effective, environmentally friendly solutions.

1.2 PROJECT AIMS

The proof-of-concept has been demonstrated at lab-scale in 4 ℓ batch tests on a synthetic sample. The proposed test-work will cover the continuous operation of the process using an industrial sample in a lab-scale pilot test treating 100 ℓ/d - 150 ℓ/d. The data from this system will form part of a high-level techno-economic valuation to predict whether the process will be economically viable and will also be used to produce design criteria for a larger-scale plant.

This study will investigate the potential of this improved two-step process at pilot-scale to produce an anticipated valuable remediation product, namely nesquehonite (a $MgCO_3$ derivative), from mine impacted solutions containing Mg. Operation at ambient or near ambient conditions may positively impact the operating costs of the process.

The specific objectives (and associated deliverables) are to:

1. Set up the pilot plant
    - Additional laboratory scale optimisation prior to piloting (Chapter 2).
    - Design set-up, procure necessary equipment and suitable sample (Chapter 3).
    - Begin continuous pilot test-work.
2. Pilot the process on a continuous basis.
    - Continuous operation with synthetic and brine samples containing Mg (Chapter 4).
3. Produce a magnesium oxide product prototype through calcination of the nesquehonite product (Chapter 5).
4. Develop a predictive model for the process application to other brine feedstocks (Chapter 6).
5. Demonstrate the financial feasibility by undertaking a desk-top economic evaluation (Chapter 7).

1.3 SCOPE AND LIMITATIONS

This project entailed piloting the mineral carbonation process continuously in a laboratory-scale pilot process, while treating an industrial brine sample from the reject brine stream from the eMalahleni Water Reclamation Plant (EWRP). The results from Mintek's previous optimisation work at laboratory-scale demonstrated that it was possible to produce two separate products of suitably high purity from an industrial brine solution using an improved, two-step mineral carbonation process. It is this new, improved "two-step" process that was piloted on a continuous basis. This project is focused exclusively on scale up from the bench tests to pilot-scale testing of the two-step process, optimisation of the various process parameters was excluded from the scope.

The study has tested the use of pure CO_2 for the mineralisation calcium and magnesium from brine. The intention for an industrial mineralisation process is to use waste CO_2 from coal-fired power plants, which likely contain traces of minor elements, especially SO_2. These compounds may interfere with the reaction or optimisation of carbon mineralisation of brines. The economic studies presented have not taken into consideration the energy consumed to maintain the temperature of the reaction at 30 °C.

CHAPTER 2: LABORATORY SCALE OPTIMISATION

2.1 INTRODUCTION

In this chapter, the optimisation of the two influential process parameters, namely the CO_2 gas flow rate and hydraulic residence time (HRT), was carried out at a laboratory scale. These variables were fine-tuned for the two-stage process that were later implemented in the pilot-scale test work. The experimental approach focussed on the reduction of CO_2 gas flow rates while simultaneously monitoring the removal of calcium and magnesium from solution. This critical step was prompted by the hypothesis that excessive CO_2 supply increased NaOH consumption (used to maintain pH at 9.5), as CO_2 decreases the solution pH via the formation of carbonic acid. Minimising CO_2 flow rate aimed to achieve maximum sequestration efficiency while reducing NaOH consumption, resulting in operational cost savings. Furthermore, optimisation of the HRT was conducted to ensure the maximal removal of calcium and magnesium in the respective stages, ensuring the production of purer products. This optimisation process involved analyses at varying flow rates and facilitated the determination of the optimum for enhanced efficiency and cost-effectiveness.

2.2 METHODS

2.2.1 Experimental setup

The laboratory-scale experiments were conducted at Mintek. The experimental apparatus (Figure 2-1) comprised a 4 ℓ glass reactor outfitted with an overhead stirrer and a hotplate to ensure accurate temperature control at 30 °C. Gas injection into the reactor was facilitated by an inline mixer, regulating CO_2 and compressed air flow rates using rotameters to achieve the desired concentrations. Continuous feeding of brine into the reactor was achieved with a peristaltic pump. Regulation of the reactor pH was maintained using a continuously operating auto-titrator, which administered 10 M NaOH when necessary. It was found that solutions in excess of 10 M NaOH were too viscous and impeded the functioning of the auto titrator.

Figure 2-1. Experimental setup of the laboratory-scale reactor

2.2.2 Optimisation work plans

During the optimisation test work, all other process conditions were kept constant to ensure the gas flow rate and HRT optimisation were independently investigated. The experimental test work campaign for the optimisation of the CO_2 gas flow rate of both stages are listed in Table 2-1. Stage 1 assessed steady-state conditions, which are typically established within approximately 1.5 hours based on prior investigations. Under these conditions, it was observed that magnesium and calcium removal rates were maintained at their maximum level. However, Stage 2 often necessitated a longer duration, typically ranging between 2.5 h to 3.0 h to achieve steady state. Subsequently, upon reaching steady-state conditions, the gas flow rate was systematically and incrementally reduced. Concurrently, calcium and magnesium concentrations were monitored. This iterative process aimed at identifying an inflection point indicative of decreased rates of magnesium and calcium removal, and thereby facilitated the determination of an optimised CO_2 consumption rate for the process. Samples were collected at 30-minute intervals and analysed for dissolved calcium and magnesium concentrations using an Atomic Absorption (AA) instrument.

Table 2-1. Incremental reduction of CO_2 gas flow rate

Time (hours)	Air flow rate (ℓ/h)	CO_2 gas flow rate (ℓ/h)	ℓ CO_2/ℓ brine/hour
		Stage 1	
0 – 2	40	15.68	3.92
2 – 3	40	13.07	3.27
3 – 4	40	11.12	2.78
4 – 5	40	8.51	2.13
5 – 6	40	6.55	1.64
		Stage 2	
0 – 3	40	16.98	5.66
3 – 4	40	11.77	3.92
4 – 5	40	8.51	2.84
5 – 6	40	6.55	2.18

The HRT of both stages was explored to achieve maximum removal of magnesium and calcium, respectively. This involved conducting three tests at different HRTs to assess their impact. During these tests, CO_2 was deliberately supplied in excess to isolate and evaluate the influence of HRT. The stages were tested at HRTs of 1.0 h, 1.3 h, and 2.0 h based on the anticipated time to reach steady state operation.

2.3 RESULTS AND DISCUSSION

2.3.1 CO_2 gas flow rate optimisation tests

Figure 2-2 and Figure 2-3 illustrate the variations in calcium and magnesium concentrations in solution for Stages 1 and 2, respectively, as CO_2 gas flow rates were incrementally reduced. In Figure 2-2, a discernible inflection point is observed for calcium (dashed red line, Figure 2-2) where dissolved calcium concentration began to rise subsequent to a reduction in CO_2 gas flow rate from 2.13 ℓ CO_2 per ℓ brine per hour to 1.64 ℓ CO_2 per ℓ brine per hour. Similarly (red dashed line, Figure 2-3), dissolved magnesium concentration exhibited an increase following a reduction in CO_2 gas flow rate from 2.84 ℓ CO_2 per ℓ brine per hour to 2.18 ℓ CO_2 per ℓ brine per hour. These findings suggest the optimised CO_2 for Stage 1 and Stage 2 to be 2.13 ℓ CO_2 per ℓ brine per hour and 2.84 ℓ CO_2 per ℓ brine per hour, respectively.

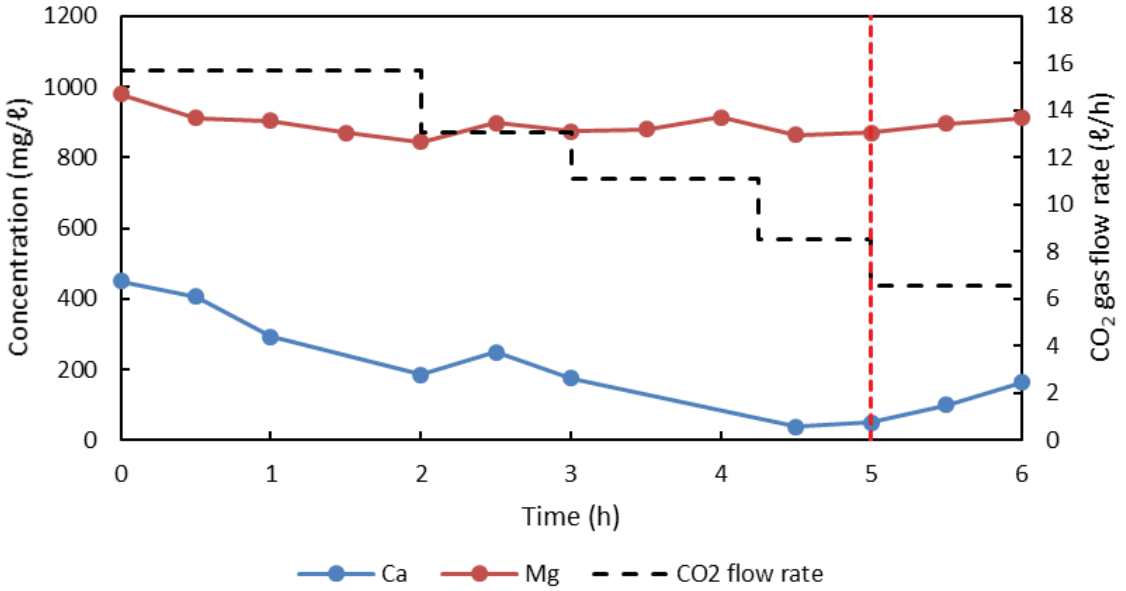

Figure 2-2. Stage 1 CO_2 optimisation: Reducing CO_2 gas flow rates while monitoring calcium and magnesium removal

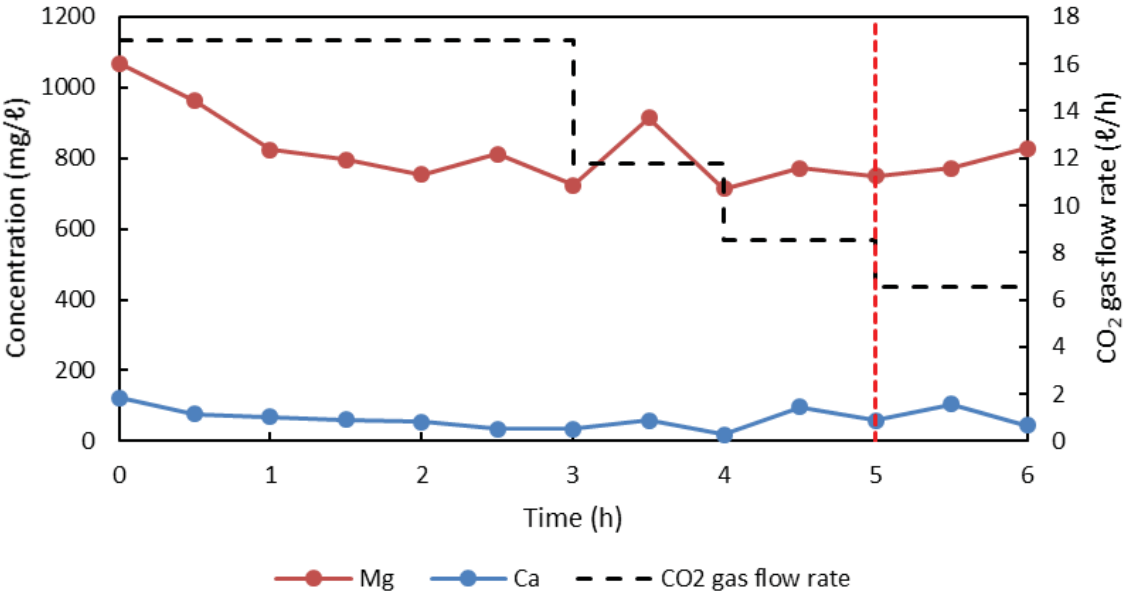

Figure 2-3. Stage 2 CO_2 optimisation: Reducing CO_2 gas flow rates while monitoring calcium and magnesium removal

2.3.2 HRT optimisation tests

The HRT optimisation tests for Stage 1 and Stage 2 are depicted in Figure 2-4 and Figure 2-5 respectively. In Figure 2-4, the concentrations of dissolved calcium and magnesium are illustrated over varying HRT values, while the corresponding removal percentages for calcium and magnesium are provided in Table 2-2. The trends observed indicate that the removal of calcium and magnesium is non-linear at lower HRTs and taper off at longer HRTs. Only the magnesium concentration curve is presented in Figure 2-5 as the calcium concentrations were below the detectible limit for the AA instrument.

To estimate the optimal HRT that corresponds to the maximum removal rate, the removal percentages of calcium for Stage 1 and magnesium for Stage 2 were plotted for comparison (Figure 2-6). Both plots suggest a parabolic fit with an apparent optimum occurring approximately 1.5 h based on the increase, peak and subsequent decrease in the data. Quadratic correlations were chosen to fit the non-linear relationship of the

data. The non-linear trends in data suggest that a linear model would not adequately represent the observed behaviour. The maximum values for these curves were calculated at 1.54 h (Stage 1) and 1.52 h (Stage 2) and represents very similar optimal HRTs of maximum removal.

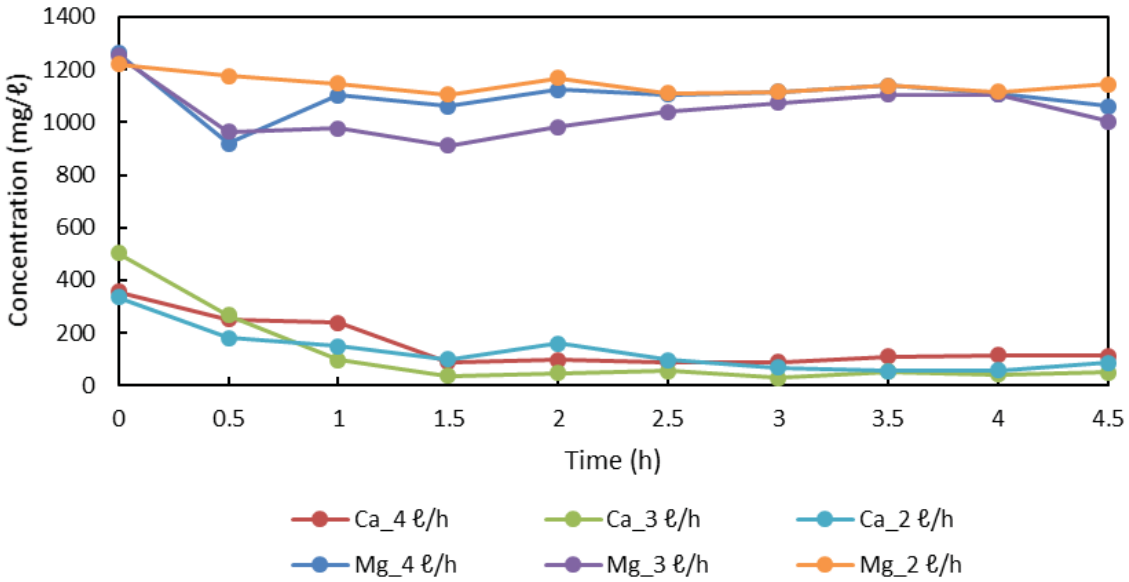

Figure 2-4. Stage 1 HRT optimisation – Comparing calcium and magnesium removal at varying HRTs

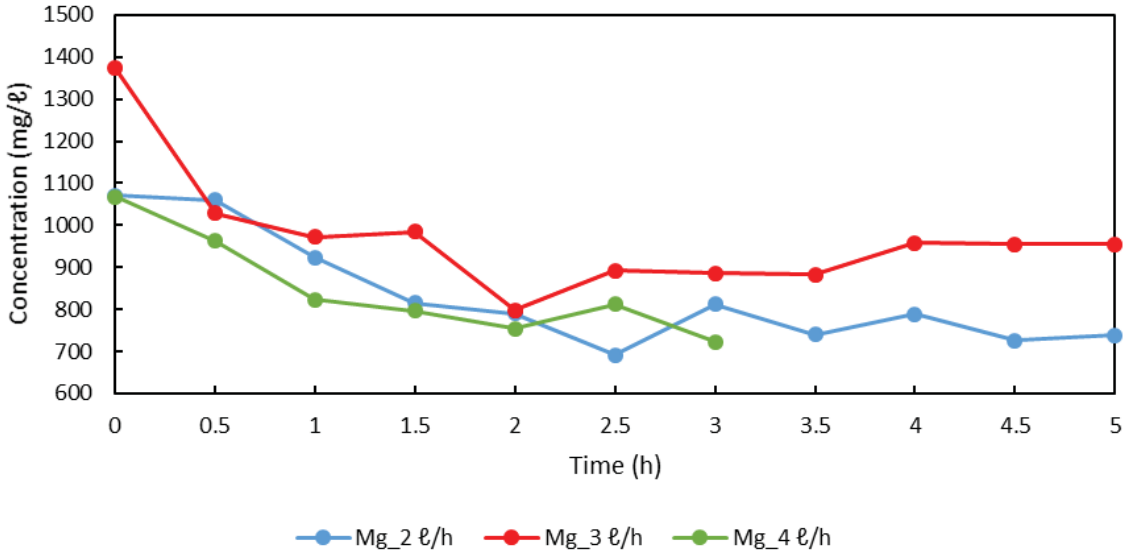

Figure 2-5. Stage 2 HRT optimisation – Comparing magnesium removal at varying HRTs

Table 2-2. Calcium and magnesium removal percentages during HRT optimisation for Stage 1 and Stage 2

HRT (hours)	Mg removal (%)	Ca removal (%)
	Stage 1	
1.0	12.72	61.07
1.3	16.64	84.66
2.0	8.94	68.32
	Stage 2	
1.0	24.00	-
1.3	32.18	-
2.0	25.47	-

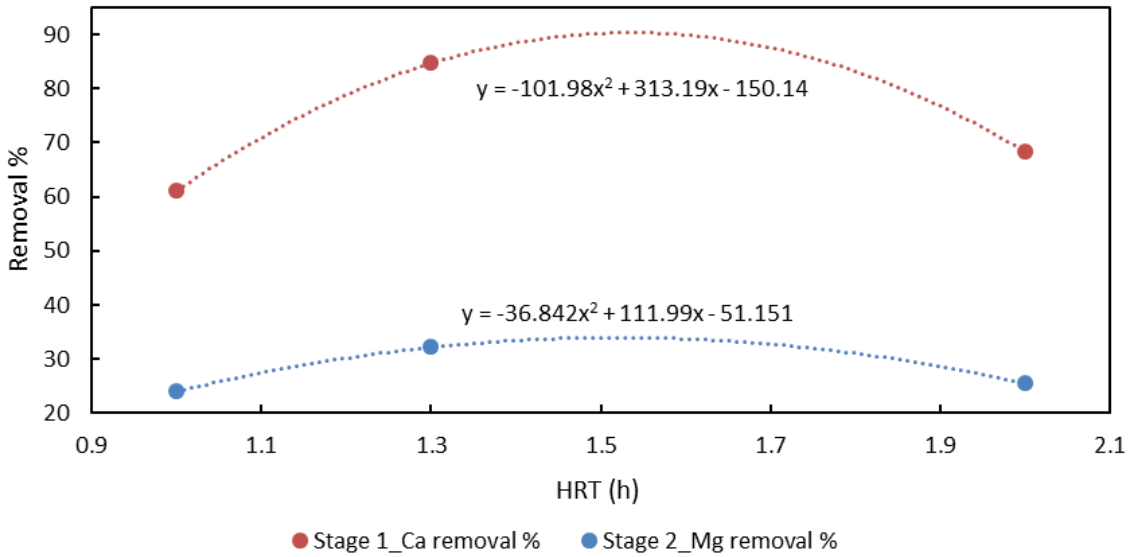

Figure 2-6. Optimisation of HRT – Stage 1 calcium removal and Stage 2 magnesium removal at varying HRT

2.4 CONCLUSION

The optimisation of the two key process parameters, namely CO_2 gas flow rate and HRT, was successfully accomplished through systematic experimentation and analysis. The findings of this study are summarised as follows:

1. CO_2 Gas Flow Rate Optimisation:
    - Stage 1: An inflection point was observed at a CO_2 feed rate of 2.13 ℓ CO_2/ ℓ brine/hour, beyond which calcium concentration in solution began to increase, indicating suboptimal removal at elevated CO_2 concentrations.
    - Stage 2: An inflection point similar to what was observed in Stage 1 was observed at 2.84 ℓ CO_2/ℓ brine/hour, where magnesium concentration increased due to inadequate CO_2 supply.
2. HRT optimisation:
    - Stage 1: Maximum calcium removal was calculated at an HRT of 1.54 hours.
    - Stage 2: Maximum magnesium removal was calculated at an HRT of 1.52 hours.

The optimisation of these critical parameters was expected to facilitate efficient and cost-effective operation of the two-stage process by maximising the removal of calcium and magnesium while minimising excessive consumption of CO_2 and NaOH which will be investigated in Chapter 4.

CHAPTER 3: PILOT PLANT SETUP

3.1 INTRODUCTION

This chapter describes the design and operational setup of a pilot plant for a brine treatment process aimed at removing calcium and magnesium ions through the improved two-stage precipitation approach. The objective of piloting this setup is to evaluate the effectiveness of the process in removing these target ions from the brine through controlled chemical precipitation. This pilot study provides a basis for understanding the operational requirements, treatment efficiencies, and product purity achieved at the pilot scale.

3.2 PILOT-PLANT PROCESS FLOW DIAGRAM

In the pilot study (Figure 3-1), brine is fed from the brine feed tank (T-1) into the first stage stirred tank reactor (R-1) at a constant flow rate using the R-1 feed pump (P-1). The reactors are equipped with hot rods (H-1 and H-2) for temperature control. Carbon dioxide is supplied from gas cylinders (G-1 and G-2) and mixed with compressed air before being introduced into the reactors. The combination of gases in-line achieves the desired gas composition prior to injection into the reactors via a sparger that used to ensure adequate dissolution of gaseous in the aqueous phase. The flow rates of the carbon dioxide and compressed air streams were controlled and monitored using rotameters installed in the gas supply lines. The pH of the reactors was maintained at 9.5 by the controlled dosing of a 10 M NaOH solution using pH control auto-titrators (AT-1 and AT-2). The process involves two consecutive stages (*i.e.*, R-1 and R-2, respectively). During the first stage (R-1), the primary aim is to remove calcium ions from the brine by precipitating them as calcium carbonate (*i.e.*, $CaCO_3$). The effluent from the first stage is filtered using a pressure filter (F-1) that separates filter cake product 1 (containing $CaCO_3$) from the liquor. The filtrate exiting pressure filter F-1 is fed into the brine feed tank (T-2), and subsequently pumped into the second stage stirred reactor (R-2) using the R-2 feed pump (P-2). In this stage, the objective is to remove Mg ions from the solution by precipitating them as nesquehonite (*i.e.*, $MgCO_3 \cdot 3H_2O$). The effluent from the second stage is filtered using another pressure filter (F-2), which produces filter cake product 2 (containing nesquehonite) and filtrate 2.

3.3 PILOT-PLANT SETUP

The pilot plant apparatus used for the experimental investigation of the two-step brine treatment process (Figure 3-2) comprises two stirred tank reactors (labelled as Stage 1 and Stage 2). Each reactor is equipped with an overhead mixer assembly and temperature control system (utilising hot rods) to maintain the desired conditions for the precipitation reactions (refer to Table 3-1). The feed streams, as well as the brine solution, carbon dioxide gas cylinders, and sodium hydroxide dosing system for pH control, were connected to the reactors through piping and tubing. CO_2 was introduced into the reactors using spargers beneath the stirrers to ensure adequate dissolution and mixing within the solution. To ensure consistent and even mixing of the CO_2 within the reactor, vertical baffles around the inside perimeter of the reactor were added, and a double Rushton impeller configuration was used for mixing. The effluent from Stage 1 was collected in a designated container before being filtered (Figure 3-2, right) and its filtrate was subsequently fed into Stage 2. Similarly, the effluent from Stage 2 was collected in its own designated container prior to undergoing filtration (Figure 3-2, right) to recover precipitated solids. The control panels and instrumentation, housed within the orange enclosures, were integrated into the pilot plant setup to monitor and regulate the stirring speed and temperature of the reactors through instrumentation and control systems. The auto-titrator system, accompanied by a computer interface, was easily accessible and was responsible for measuring, monitoring and controlling the pH of the reactors by dosing sodium hydroxide solution.

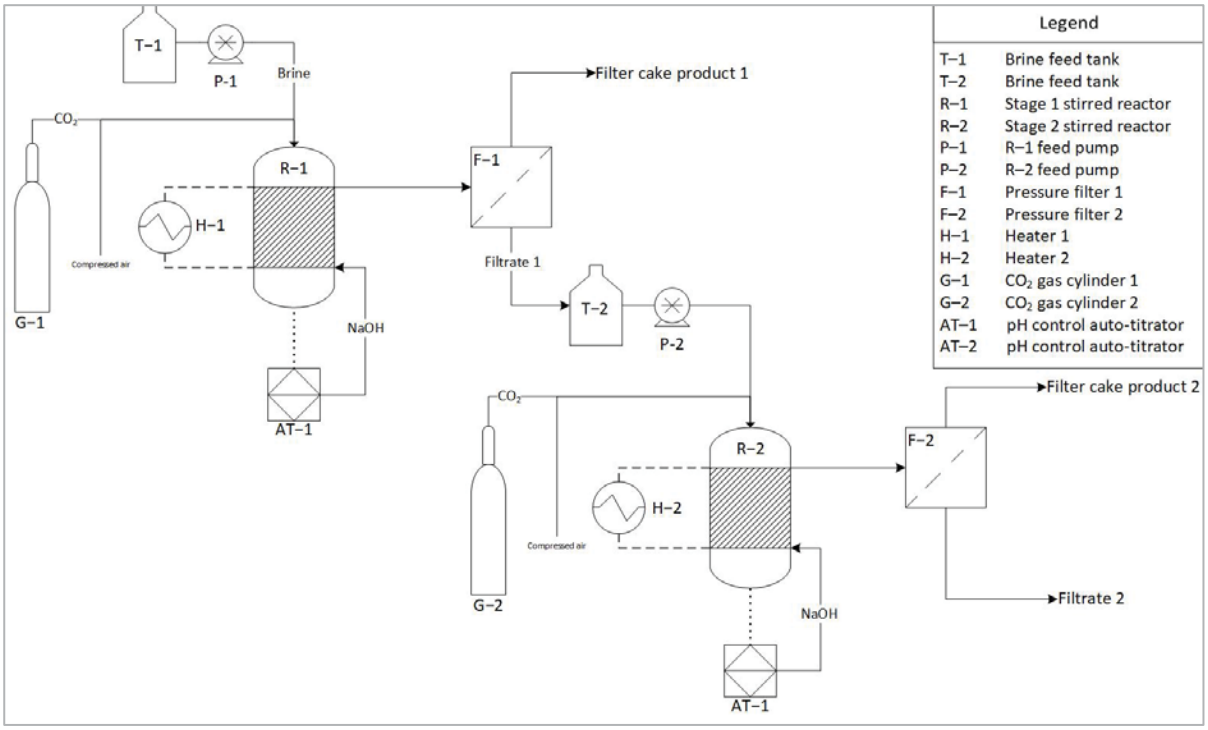

Figure 3-1. Process flow diagram of pilot-plant

Figure 3-2. Photographs of the pilot-plant setup (left), and the filter press (right)

3.4 PILOT-PLANT OPERATION CONDITIONS

3.4.1 Baseline operating conditions

To establish a baseline understanding of the process at pilot-scale, two feedstocks were formulated using industrial brine sample obtained from eMalahleni Water Reclamation Plant (EWRP) as the make-up feedstock. The feedstock was formulated either with or without magnesium dosing to above 1 g/ℓ with $MgSO_4$, so as to compare the behaviour between the elevated concentrations, since previous studies indicated that the magnesium concentrations in the solution needed to exceed 1 g/ℓ to achieve adequate removal for product formation. During the test work, the process was piloted using the baseline operating conditions obtained from previous work conducted by Mintek, as detailed in Table 3-1.

Table 3-1. Baseline pilot operating conditions

pH	Temperature (°C)	NaOH titrant (M)	Feed flow rate (ℓ/h)	Gas flow rate (ℓ/h)	CO_2 %	Stirrer speed (rpm)
9.5	25-30	15	20	400	20	250

3.4.2 Optimised operation conditions

To gather data necessary for assessing the feasibility of the process, an optimised pilot plant was operated to obtain valuable insights into product recovery, product purity, and process operation. These findings were utilised to conduct a techno-economic assessment. The optimised gas flow rate and HRT (Table 3-2) were determined by using the findings laboratory-scale optimisation tests, as outlined in Chapter 2. The brine obtained from EWRP was dosed with $MgSO_4$ to ensure that Mg concentrations remained above 1 g/ℓ for all tests.

Table 3-2. Pilot-plant process conditions

Stage 1		
Process parameter	**Value**	**Unit**
Reactor operating volume	22.7	ℓ
HRT	1.5	h
Brine feed flow rate	15.1	ℓ/h
Temperature	30	°C
Total gas flow rate	454	ℓ/h
CO_2 % (v/v)	8.26	%
ℓ CO_2/ ℓ brine/hour	2.13	-
Stirring speed	250	rpm
Stage 2		
Reactor operating volume	22.7	ℓ
HRT	1.5	h
Brine feed flow rate	15.1	ℓ/h
Temperature	30	°C
Total gas flow rate	454	ℓ/h
CO_2 %	9.34	%
ℓ CO_2/ ℓ brine/hour	2.84	-
Stirring speed	250	rpm

CHAPTER 4: PILOT PLANT OPERATION

4.1 INTRODUCTION

This section details pilot plant runs that establish the baseline operating conditions for the carbonation of brine feedstocks. The objective is to evaluate the operability of the two-stage carbonation system using both raw and dosed brine samples, which facilitates a comprehensive understanding of the system's efficiency in removing calcium and magnesium. By systematically assessing the removal rates of these metals, the study aims to identify key factors influencing carbonation dynamics, including the effects of chemical composition, competing ions, and carbonate precipitation behaviours. The focus of this analysis is on establishing baseline performance metrics that serve as a reference for subsequent optimisations and pilot tests. Additionally, the impact of seeding with nesquehonite and variations in sulphate concentrations on metal removal efficiencies will be examined. These baseline runs are critical for developing a robust understanding of the carbonation process, ultimately guiding the optimisation of conditions that enhance CO_2 sequestration and improve overall process feasibility. This foundational work will pave the way for subsequent evaluations of the process's scalability and economic viability.

4.2 BASELINE PILOT RUNS: ESTABLISHING PROCESS NORMS

4.2.1 Stage 1 pilot operation aqueous phase analysis

The removal of calcium during Stage 1 is similar for raw and dosed brine feedstocks (Figure 4-1). While the concentration of magnesium for the raw feedstock remains stable during Stage 1, some moderate removal occurs for the dosed feedstock. Rates of removal for the calcium associated with the raw feedstock tend towards 100 % from an HRT of 2.5 h (Figure 4-2). Removal rates for calcium associated with the dosed feedstock is somewhat inhibited although the removal response is quicker and achieves a removal rate above 80 % after 1.0 h, compared to the raw feedstock. The highest removal rates for calcium were found to be 100.0 % (raw feedstock) and 96.6 % (dosed feedstock). These results also demonstrate a reproducible consistency in sufficient removal of calcium between the two feedstocks.

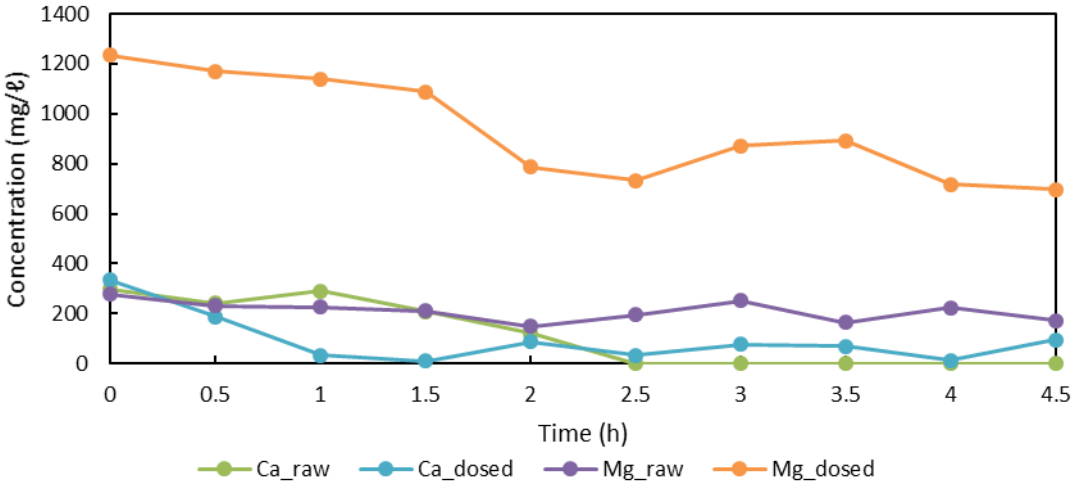

Figure 4-1. Baseline process operating conditions for magnesium and calcium Stage 1 concentrations

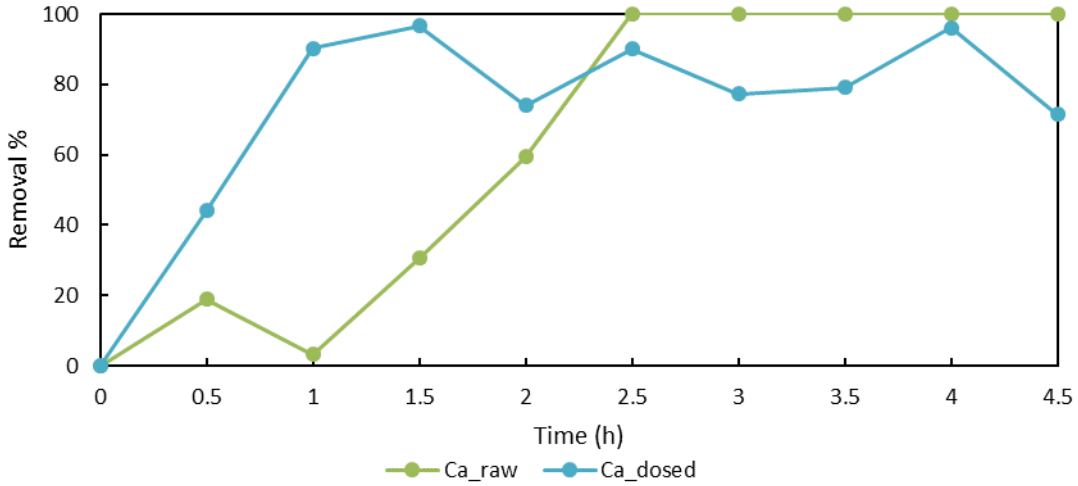

Figure 4-2. Calcium removal percentages for different feedstocks in the Stage 1 pilot runs

In contrast to calcium removal, Stage 1 treatment of magnesium feedstocks presented fluctuations in removal rates (Figure 4-3). While initially comparable, the raw brine failed to sustain stable removal rates compared to what was achieved by the dosed brine, with both feedstocks approaching 50 % removal rates from 2.0 h onwards. The variability observed in magnesium removal highlights the intricate nature of the brine treatment process. Factors such as the presence of competing ions and the dynamics of carbonate precipitation reactions play pivotal roles in influencing the efficacy of magnesium removal (Choi *et al.*, 2023). This complexity underscores the necessity of employing a two-stage process to address these challenges effectively.

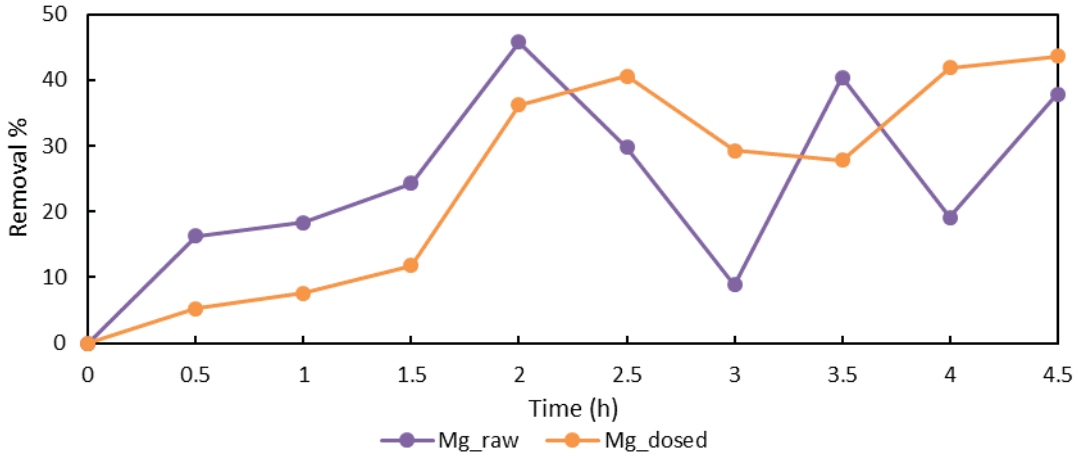

Figure 4-3. Magnesium removal percentages for different feedstocks in the Stage 1 pilot runs

4.2.2 Stage 1 pilot operation solid phase analysis

A comparison of precipitate masses and their associated production rates (Table 4-1) shows that the dosed brine achieved the highest product production rate with respect to total precipitates at 134.18 g/h compared to the raw brine (41.40 g/h). This trend emphasises the influence of the distinctive chemical composition of the brine on the efficacy of CO_2 sequestration through mineralisation. While similar magnesium removal percentages were observed, the increased concentrations associated with the dosed brine translated to significant increases for magnesium removal (13.40 %) and production rates (17.98 g/h) compared to the raw brine. The calcium removal percentage of the raw brine (36.9 %) was elevated above that of the dosed brine (13.2 %), which was attributed to elevated sulphate concentrations and the competition between calcium and magnesium precipitation reactions. These findings support the assumption that optimal removal efficiency requires magnesium concentrations ideally exceeding 1 000 mg/ℓ to maximise CO_2 sequestration rates through enhanced precipitation driving forces.

Table 4-1. Stage 1 pilot operation product mass and production rate

Feedstock	Mass precipitate (g)	Precipitate production rate (g/h)	Ca mass%	Ca removal rate (g/h)	Mg mass%	Mg removal rate (g/h)
Raw brine	207.00	41.40	36.9	15.28	1.30	0.54
Dosed brine	603.79	134.18	13.2	17.71	13.40	17.98

4.2.3 Stage 2 pilot operation aqueous phase analysis

Magnesium concentration during Stage 2 treatment of the dosed feedstock initially decreased with increasing HRT up to 0.5 h and thereafter become stable (Figure 4-4). The Stage 2 treatment of raw magnesium showed a slight decrease in magnesium concentration with increasing HRT of up to 3.0 h. Calcium concentration following Stage 2 treatment showed a decrease with respect to the raw feedstock (concentrations from 2.0 h onwards were below the detectible limit of the AA instrument), while the calcium concentration for the dosed feedstock showed little response to Stage 2 treatment.

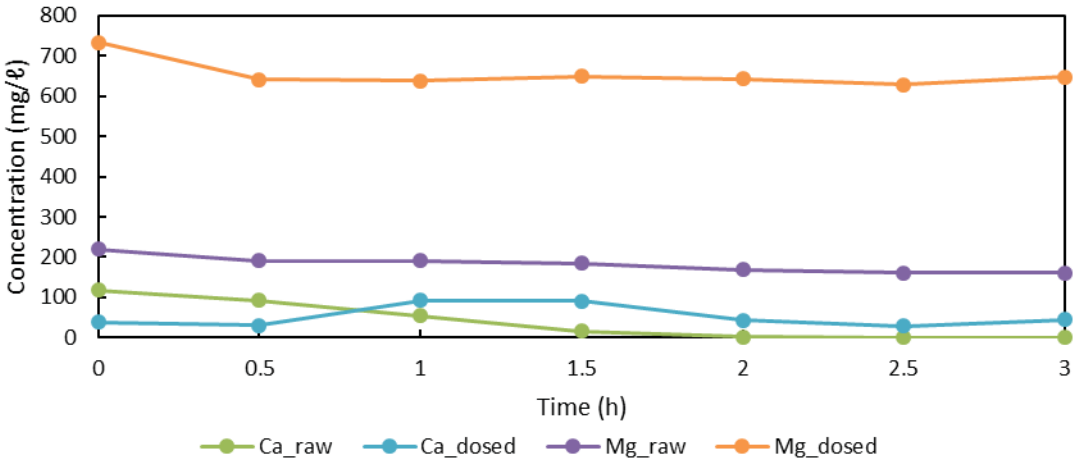

Figure 4-4. Baseline process norms for magnesium and calcium concentrations in Stage 2 pilot runs

Stage 2 treatment of raw feedstock shows a slightly higher removal percentage of 34.3 % (Figure 4-5) compared to the dosed feedstock (28.2 %). The decline in removal in the dosed test suggests a potential interference due to increased sulphate concentrations from the $MgSO_4$ added to increase the magnesium concentration (refer to 4.2.5). The magnesium removal percentages obtained from the baseline pilot operation were akin to the results acquired during the optimised 4 ℓ lab scale tests, where the maximum removal achieved approached the 25 % to 30 % range (detailed in Table 2-2 of Chapter 2). The overall agreement between results supports the scalability of the process.

The removal rate of magnesium is consistently higher in the raw feedstock reactor compared to the non-dosed feedstock reactor. However, it should be stressed that the concentration of magnesium in the raw feedstock is significantly lower, at 200 mg/ℓ, compared to the dosed feedstock (800 mg/ℓ). As a result, despite the lower removal efficiency observed in the dosed reactor, the overall amount of precipitate collected is greater from the dosed feedstock due to its elevated concentration of magnesium. This highlights the influence of initial concentration on the quantity of precipitate generated, even though the removal rates in the dosed system are lower.

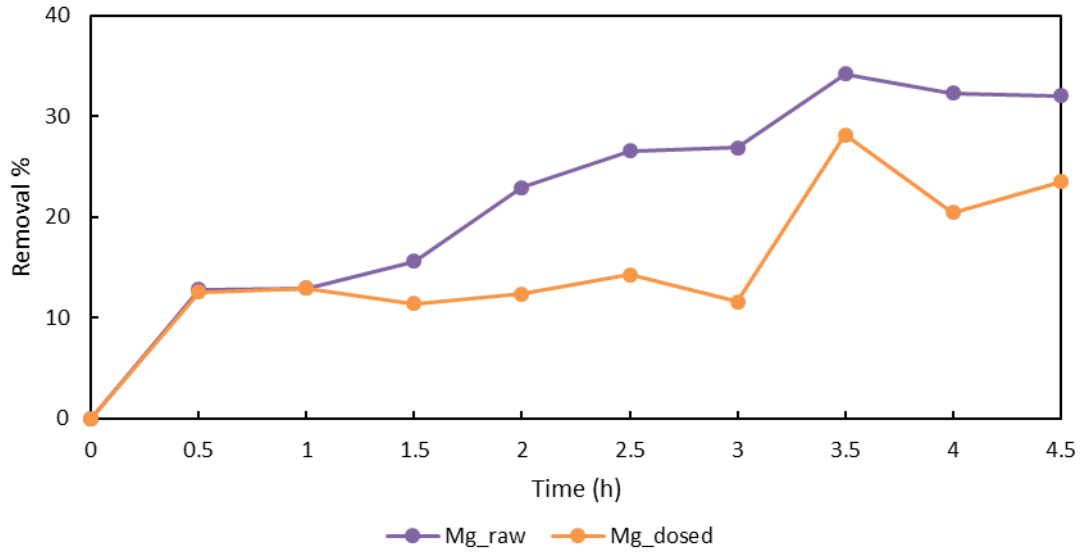

Figure 4-5. Magnesium removal percentages for different feedstocks in the Stage 2 pilot runs

4.2.4 Stage 2 solid phase analysis

The dosed brine feedstock produced a significantly higher total mass of precipitate compared to the raw brine feedstock (Table 4-2). This translated to a much higher precipitate production rate for the dosed brine at 13.71 g/h compared to 2.90 g/h for the raw brine. The magnesium mass percentage in the precipitate was markedly higher for the dosed brine at 16.2 % compared to just 1.6 % for the raw brine precipitate. Consequently, the magnesium removal rate was substantially elevated for the dosed brine at 1.55 g/h, over 30 times higher than the 0.05 g/h rate achieved with the raw brine feedstock. These results clearly demonstrate the beneficial impact of elevated concentrations of magnesium in the brine for feasible recovery and efficient CO_2 sequestration.

Table 4-2. Stage 2 pilot operation product mass and production rate

Feedstock	Mass precipitate (g)	Precipitate production rate (g/h)	Mg mass%	Mg removal rate (g/h)
Raw brine	14.50	2.90	1.6	0.05
Dosed brine	47.99	13.71	16.2	1.55

4.2.4.1 Effect of seeding on Stage 2 product yield

Historical work by Mintek showed that seeding Stage 2 with nesquehonite can improve product yield by around 450 %. To investigate the impact on magnesium removal rates, two pilot-scale dosed brine Stage 2 tests were conducted—one with seeding and one without seeding. The magnesium concentrations of the feed for each of the tests were 996 mg/ℓ, and 881 mg/ℓ for the seeded tests. For the seeded test, nesquehonite seed crystals were initially added at 100 g per 22.7 ℓ of operating volume in the reactor to provide sufficient nucleation sites for crystal formation. At the end of the 2.5-hour test period, the seeded run achieved around 29 % magnesium removal rate, which is significantly higher than the 11 % removal attained in the unseeded run (Figure 4-6). The non-linear increase in magnesium removal for the seeded run suggests that removal rates may increase with increasing HRT post 2.5 h. The enhanced magnesium removal performance in the seeded run can be attributed to the introduction of nesquehonite seed crystals, which provided additional nucleation sites for precipitation. This seeding facilitated heterogeneous nucleation, which was found to accelerate the precipitation kinetics and enabled more rapid magnesium capture from the brine solution. However, further investigation into the effect of seeding on long-term magnesium removal using optimised pilot runs will be carried out in future work to determine its effectiveness over an extended period of operation.

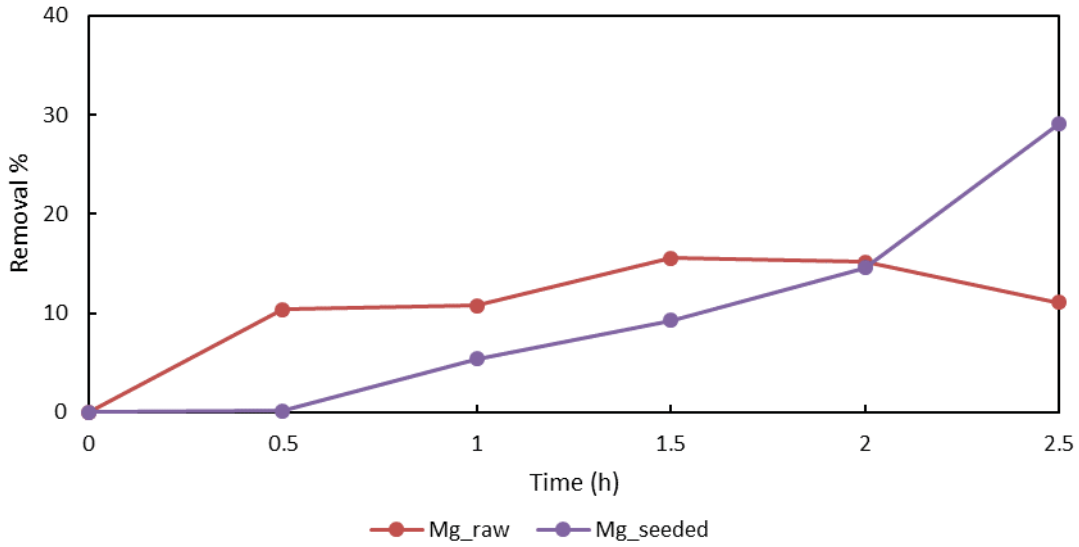

Figure 4-6. Effect of nesquehonite seeding on Mg removal during Stage 2 pilot operation

4.2.5 Impact of sulphate concentrations on mineral precipitation

Further experimental work on synthetic solutions and diluted brines was undertaken to illustrate the effect of elevated sulphate concentrations (at 5.2 g/ℓ, 8.0 g/ℓ and 16.0 g/ℓ) on magnesium and calcium removal. The fixed experimental conditions were as follows: pH controlled at 9.5; CO_2 controlled at 20 %; ambient temperature and pressure employed; total gas flow rate (at 80 ℓ/h); NaOH titrant (15 M) and constant stirrer speed (250 rpm). A synthetic solution was formulated as the model feedstock, which included 1.0 g/ℓ magnesium and 0.5 g/ℓ calcium.

The presence of elevated sulphate concentrations above the 5.2 g/ℓ sulphate baseline had a significantly negative effect on magnesium removal via mineral carbonation. Magnesium removal decreased from 57 % at 5.2 g/ℓ sulphate to 40 % at 8.0 g/ ℓ, and even further to just 17 % at 16.0 g/ℓ sulphate over the 5.0-hour duration of assessment (Figure 4-7). A lesser but notable effect was observed for calcium, with the maximum removal rate decreasing from 90 % at 5.2 g/ ℓ sulphate to 85 % at 8.0 g/ℓ and 78 % at 16.0 g/ℓ after 5 hours. This 7 % to 12 % reduction contrasted with the > 40 % decline in magnesium removal and highlights the more pronounced inhibitory impact of sulphate on magnesium carbonation compared to calcium.

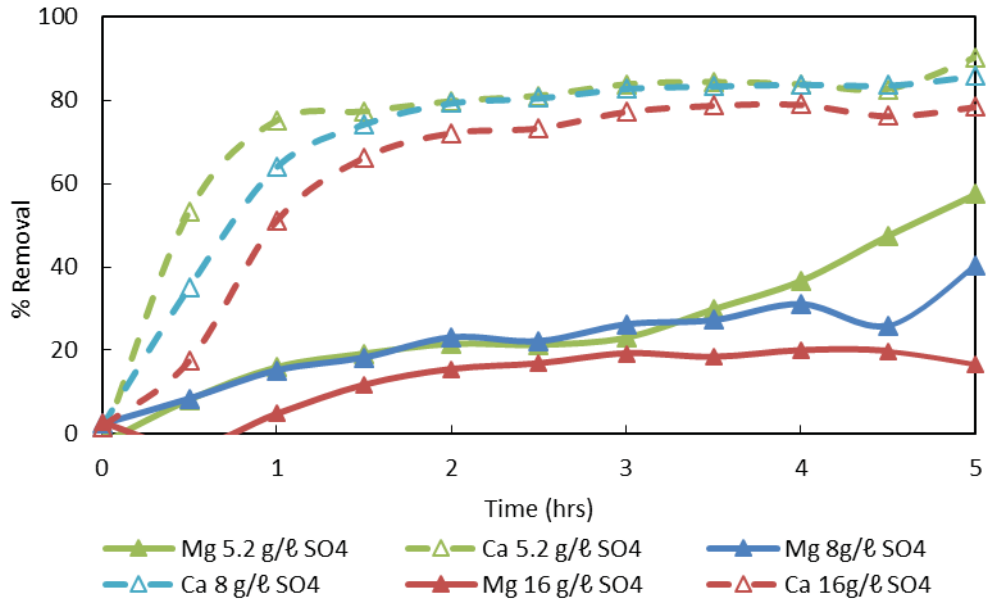

Figure 4-7. Impact of elevated sulphate concentrations on magnesium and calcium removal potential

4.3 STEADY STATE OPTIMISED PILOT OPERATION – STAGE 1

4.3.1 Brine feed composition – Stage 1

The initial brine composition was analysed using Inductively Coupled Plasma (ICP) spectroscopy (Table 4-3). The brine is characterised by high concentrations of sodium and significant levels of magnesium and calcium. The presence of other elements in lower concentrations, particularly aluminium, iron, lithium, manganese, nickel, silica and zinc, speaks to the complexity of the brine composition.

Table 4-3. Brine feed composition

Concentration (mg/ℓ)										
Na	Al	Ca	Fe	Mg	Li	Mn	Ni	Si	Zn	SO_4
19 300	0.13	506	1.18	1240	37.80	2.64	1.17	2.38	0.41	36 000

4.3.2 Aqueous results – Stage 1

A comparison of magnesium and calcium concentrations (Figure 4-8) and removal rates (Figure 4-9) following duplicate Stage 1 treatments was used to evaluate the process potential under steady-state conditions. The process reached steady state after 5 hours of operation with respect to magnesium removal (which corresponds to approximately 3 volume cycles—a behaviour consistent with rule-of-thumb characteristics), after partial steady state was achieved with respect to calcium removal (at 2.5 h). The calcium removal percentages peaked at 81 % (Run 1) and 88 % (Run 2). Concurrently, magnesium removal peaked at around 50 % for both runs. These lower removal rates compared to previous baseline runs are likely attributed to the introduction of a new brine feedstock characterised by markedly higher sulphate concentrations of 34.2 g/ℓ (Run 1) and 36.0 g/ℓ (Run 2) compared to 15.4 g/ℓ. In the baseline runs. The elevated sulphate levels appear to have adversely affected removal efficiencies, and lead to a decrease of approximately 10 % to 15 % relative to the baseline tests.

These findings underscore the critical influence of brine composition, specifically sulphate concentrations, on the efficacy of mineral carbonation processes. Elevated sulphate levels impeded precipitation reactions, thereby compromising the efficient removal of calcium and magnesium ions from solution. While magnesium removal exhibited greater resilience, achieving approximately 50 % capture across both runs. The substantial reduction in calcium removal rates under heightened sulphate conditions highlights the imperative for robust sulphate management strategies. Such strategies are essential to optimise overall process efficiency and sustain consistently high removal rates for both target ions in mineral carbonation applications.

Figure 4-10 shows that, initially for Run 1, NaOH consumption rates remained steady up until 4.5 h. However, beyond this time, substantial increases in NaOH consumption were observed. This uptick can be attributed to enhanced CO_2 addition, which necessitates higher NaOH dosages to maintain the reactor pH setpoint level. A similar pattern emerged in the magnesium removal dynamics of Run 1, where after 4.5 hours, there was a discernible increase in removal efficiency. This suggests that the CO_2 dosage in Run 1 after 1 hour of operation decreased as seen from the NaOH dosage, together with an associated reduction in Mg removal (Figure 4-9). Subsequently, NaOH dosage was increased by the operators of the plant after 4.5 hours of operation. The trend observed in Figure 4-9 for calcium suggests that calcium preferentially reacts over magnesium as the removal rate of calcium was unaffected by the changes in CO_2 and NaOH, and magnesium only showed an increase of removal after the CO_2 was increased. The NaOH consumption presented in Figure 4-10 was calculated as the average across the two runs, which equated to 760 mℓ NaOH/ hour (at 10 M) operating at 1.5 h HRT. This averaged value was used for the techno-economics evaluation (refer to Section 6.3)

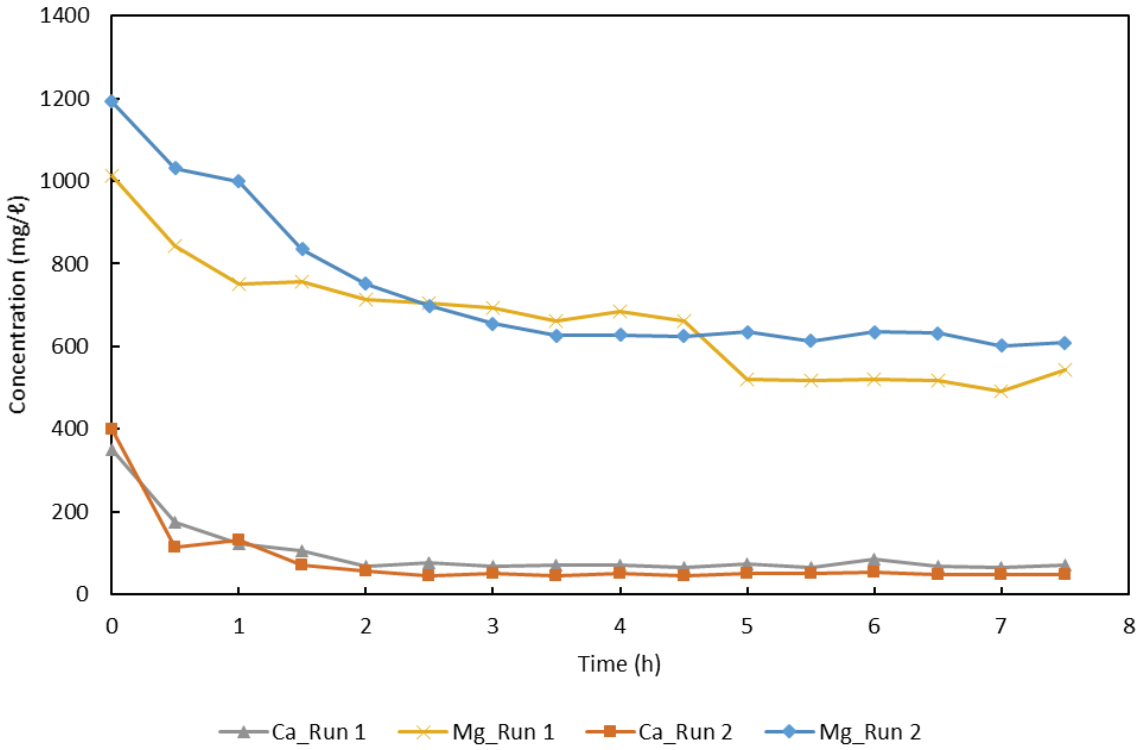

Figure 4-8. Calcium and magnesium concentrations in solution during stage 1 pilot plant operation

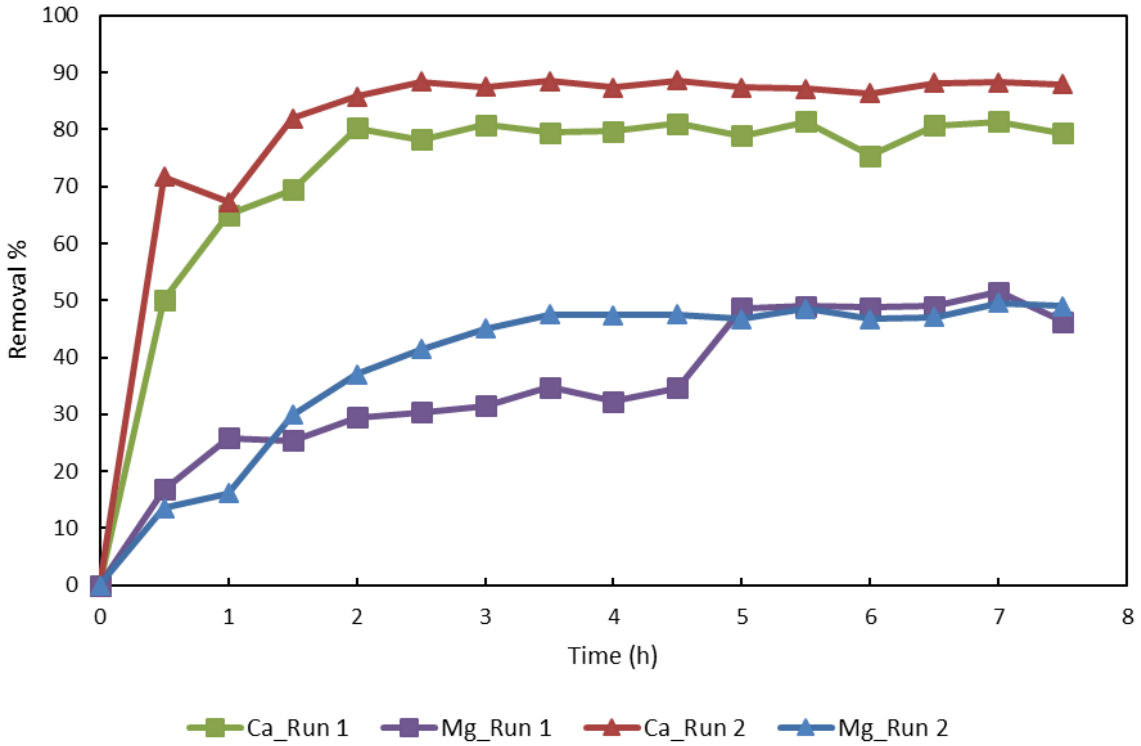

Figure 4-9. Calcium and magnesium removal percentages optimised pilot operation

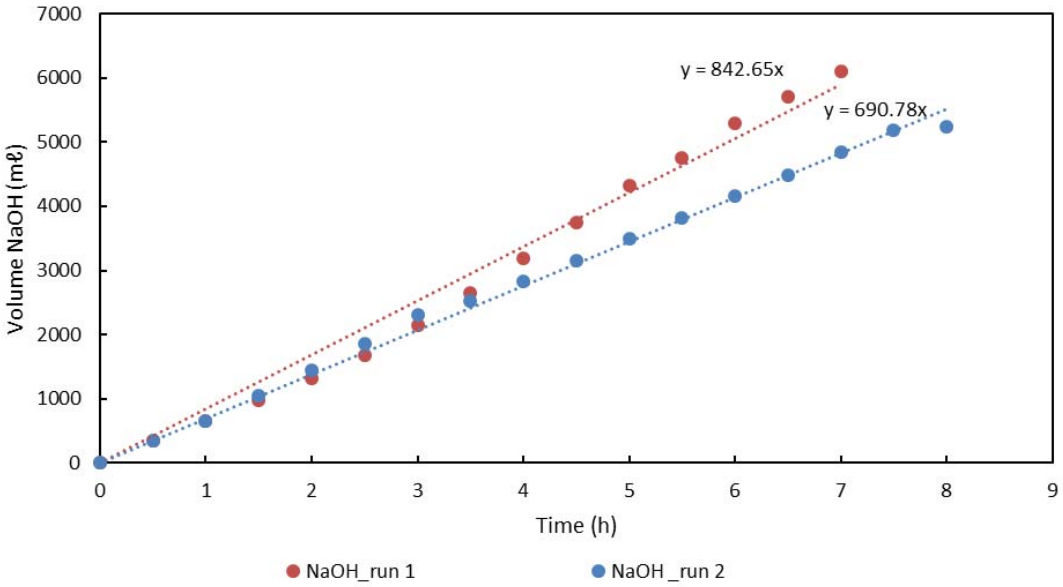

Figure 4-10. NaOH consumption rates during Stage 1 pilot runs

4.3.3 Solid characterisation results – Stage 1

The cumulative precipitate production (Table 4-4) was consistent for Run 1 (at 617.74 g) and Run 2 (619.19 g), with corresponding production rates of 82.37 g/h (Run 1) and 77.40 g/h (Run 2). The calcium content in the precipitate remained relatively stable, with mass percentages of 11.9 % (Run 1) and 12.6 % (Run 2), and removal rates of 9.75 g/h (Run 1) and 9.80 g/h (Run 2). Notably, a slight increase in magnesium content was observed from 6.79 % to 8.25 %, accompanied by an increase in removal rates of 5.59 g/h to 6.38 g/h between the Run 1 and Run 2. This increase was attributed to elevated magnesium concentrations in the feed (1013 mg/ℓ and 1192 mg/ℓ), facilitating a higher rate of reaction.

A comparison with the baseline dosed brine run presented in Table 4-1 suggests diminished mineral removal efficiencies in the optimised runs. These reduced removal rates were attributed to the increased sulphate concentrations during the optimised runs, the impact of which is further elucidated to in Figure 4-7.

Table 4-4. Stage 1 product classification and production rates

Run	Total precipitate mass (g)	Precipitate production rate (g/h)	Ca mass%	Ca removal rate (g/h)	Mg mass%	Mg removal rate (g/h)
1	617.74	82.37	11.9	9.80	6.79	5.59
2	619.19	77.40	12.6	9.75	8.25	6.38

The Stage 1 carbonation process aimed to remove calcium and produce a mixed product while preserving magnesium in solution for the subsequent processing in Stage 2. A comparison of the feed brine composition with the XRD results (Table 4-5) with respect to the carbonation products shows several significant findings. Firstly, the formation of monohydrocalcite (at 30.20 % for Run 1 and 39.60 % for Run 2) indicates effective calcium removal from the brine by this route. The higher monohydrocalcite content in Run 2 confirms the increased removal of calcium in Run 1 compared to Run 2 as observed in Figure 4-9. Secondly, the presence of tychite in both runs, albeit decreasing from 13.08 % to 5.70 %, demonstrates the incorporative utilisation of sodium from the brine. This is consistent with the high sodium content (19 300 mg/ ℓ) observed in the feed, which suggests that the precipitation mechanism may be more complex than initially anticipated. Although sodium typically remains soluble at the overall reaction pH of 9.5, the precipitation of sodium could stem from localised zones of elevated pH near the points where NaOH is dosed into the reactor. The reduction in tychite content of Run 2 compared to Run 1 directly correlates with differences in NaOH loading rates between the

two runs (Figure 4-10). The presence of various aluminosilicate phases (*i.e.*, natrolite, palygorskite, clinoptilolite) in Run 2 indicates that even low concentrations of aluminium (0.13 mg/ ℓ) and silicon (2.38 mg/ ℓ) in the feed brine, combined with elevated NaOH dosing, can promote the formation of sodium-rich aluminosilicates. This was evident in the formation of natrolite in Run 1 (at 11.61 %) and its absence in Run 2 (where NaOH dosing was reduced).

Table 4-5. Stage 1 precipitate XRD speciation results

Mineral	Ideal Chemical Formula	Abundance (%)	
		Run 1	Run 2
Nesquehonite	$Mg(HCO_3)(OH)•_2(H_2O)$	31.11	48.70
Monohydrocalcite	$Ca(CO_3)•(H_2O)$	30.20	39.60
Clinoptilolite	$(Ca,Na,K)_2$-$3Al_3(Al,Si)2Si_{13}O_{36}•12(H_2O)$	-	5.00
Tychite	$Na_6Mg_2(CO_3)_4(SO_4)$	13.08	5.70
Calcite	$CaCO_3$	0.33	0.40
Anhydrite	$Ca(SO_4)$	4.27	0.60
Murmanite	$(Na,[\ ])_2\{(Na,Ti)_4[Ti_2(O,H_2O)4Si_4O_{14}](OH,F)_2\}•2H_2O$	5.94	-
Natrolite	$Na_2Al_2Si_3O_{10}•2(H_2O)$	11.61	-
Palygorskite	$(Mg,Al)_2Si_4O_{10}(OH)•4(H_2O)$	3.46	-

The experimental mass percentages for calcium (10.56 % for Run 1 and 11.51 % for Run 2) and magnesium (5.55 % for Run 1 and 7.86 % for Run 2) in the precipitates were founded to be consistently lower than anticipated when compared to the mass percentages of calcium (11.64 % for Run 1 and 13.93 for Run 2) and magnesium (6.99 % for Run 1 and 9.10 % for Run 2) associated with the mass percentage characterisations (Table 4-6). These discrepancies suggest the occurrence of secondary reactions within the product vessel, potentially augmenting the total precipitate mass and thereby diluting the relative percentages of calcium and magnesium vis-à-vis the aqueous data for mineral removal.

Table 4-6. Metal balance accountability – Stage 1

Run	Mass precipitate (g)	Element	Mass percentage Experimental	Mass percentage Characterisation	Accountability (%)
1	617.74	Ca	10.56	11.64	89.76
		Mg	5.55	6.99	74.09
2	619.19	Ca	11.51	13.93	78.94
		Mg	7.86	9.10	84.17

4.4 STEADY STATE OPERATION – STAGE 2

4.4.1 Aqueous results – Stage 2

The aqueous concentrations of magnesium and calcium were measured over the course of the two 6- and 7-hour runs (Figure 4-11) and continued thereafter until the available feed from Stage 1 was depleted. Seeding was uniformly applied in both runs to stimulate precipitation and enhance removal rates. The calcium concentrations in the aqueous phase remained constant throughout the operation, indicating limited potential for further removal from solution at lower concentrations. Magnesium concentrations were only marginally reduced up until 1.0 h and remained stable thereafter. Removal rates for magnesium peaked at approximately 26 % for Run 1 and 24 % for Run 2 within the first 2-3 hours of operation (Figure 4-12). The initial peak in magnesium removal rates, followed by a decline to a steady-state value, is most likely due to the saturation of reactive sites and changes in solution chemistry that occur as magnesium is removed from the solution.

Therefore, while seeding proves beneficial, its efficacy may be constrained in the presence of elevated sulphate levels, which necessitates additional process adjustments or pre-treatment measures to mitigate sulphate interference effectively.

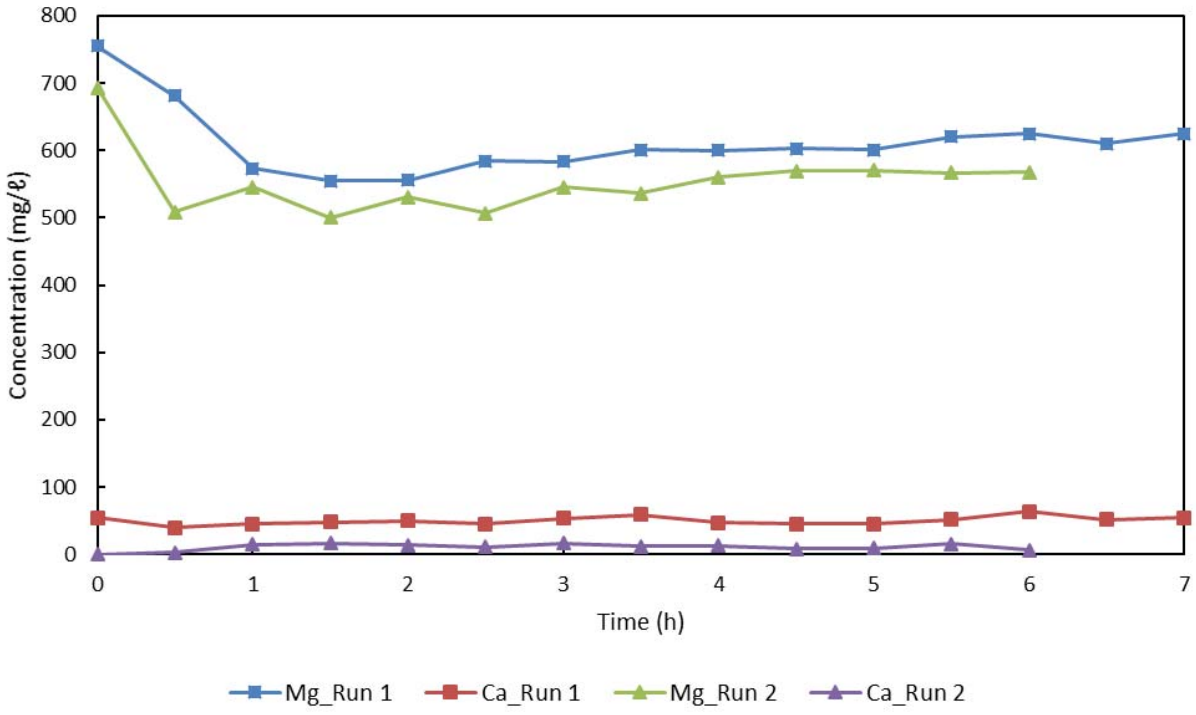

Figure 4-11. Calcium and magnesium concentrations in solution during stage 1 pilot plant operation

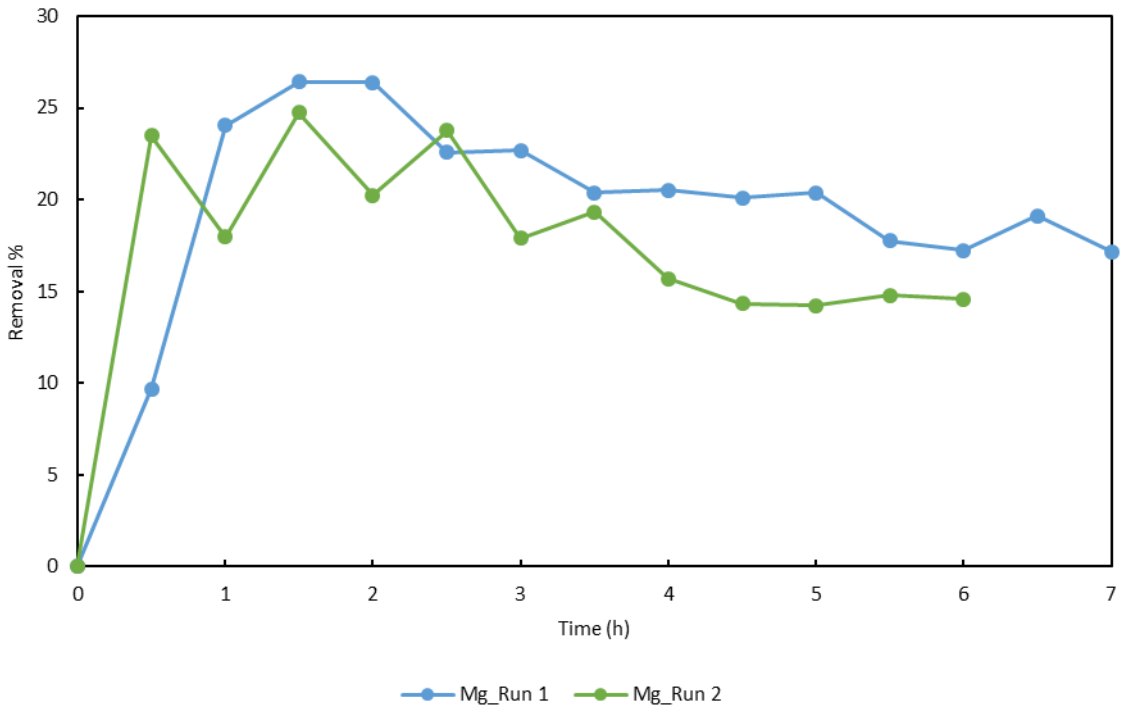

Figure 4-12. Magnesium removal percentages during Stage 2 optimised pilot operation

NaOH consumption data (Figure 4-13) shows a considerable deviation between the two runs, where NaOH consumption during Run 2 decreased substantially compared to Run 1. This reduction in NaOH consumption during Run 2 was primarily attributed to a drop in pressure within the CO_2 feed lines, which subsequently reduced the flow rate through the rotameters, thereby decreasing the overall gas flow rates. Furthermore, Run 2 showed decreased removal efficiencies of magnesium. Due to this reduction in gas flow, the NaOH consumption rate of 635 mℓ of 10 M NaOH per hour observed in Run 1 will serve as the basis for the techno-economic assessment of the process. This standardised consumption rate ensures consistency in evaluating operational costs and efficiency metrics across different process conditions and scenarios.

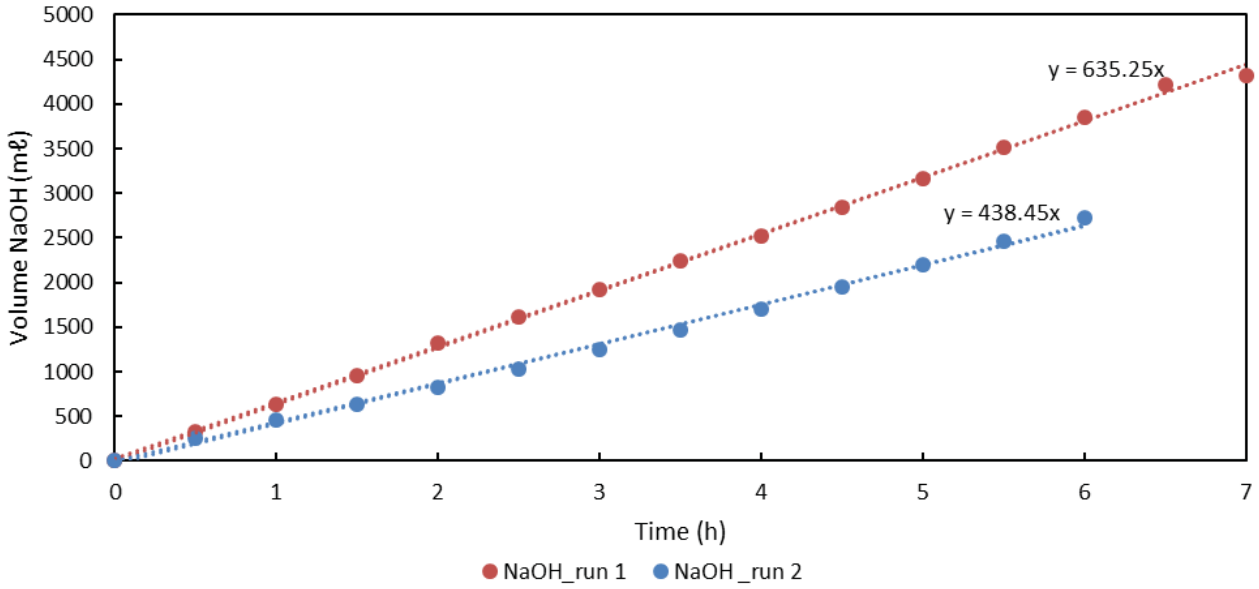

Figure 4-13. NaOH consumption rate during Stage 2 pilot runs

4.4.2 Solid characterisation results – Stage 2

Table 4-7 presents the data from the two duplicate stage 2 runs, where the majority of calcium in the feed brine was precipitated during Stage 1, followed by the production of a high-purity magnesium carbonate during Stage 2. Each run's data includes total precipitate mass produced (excluding 100 g seeding), precipitate production rates, calcium and magnesium mass percentages in the precipitate, and their respective removal rates. The reduced precipitate production (69.84 g at 10.91 g/h) and magnesium removal rates (16.3 % at 1.78 g/h) observed in Run 2 are attributed to the decrease in CO_2 gas flow rate supplied to the reactor, as indicated by the highly reduced dosing of NaOH (Figure 4-13). This suggests that Run 2 operated under suboptimal conditions that resulted in its diminished performance.

The favourable performance of Run 1 compared to the baseline runs (Table 4-2) underscores the effectiveness of seeding in enhancing the precipitation process. The optimised run achieved a precipitate production rate of 17.56 g/h, which was 28 % higher than those in the baseline rate of 13.71 g/h. This improvement suggests that seeding enhanced precipitate formation by providing nucleation sites for carbonate solid formation. Furthermore, the optimised runs demonstrated higher magnesium removal rates (2.58 g/h and 1.78 g/h) compared to the baseline runs (0.05 g/h and 1.55 g/h), even with the reduced CO_2 dosage in Run 2. This highlights the efficacy of seeding in improving magnesium removal efficiency.

Table 4-7. Stage 2 product classification and production rates

Run	Mass precipitate (g) (minus 100 g seeding)	Precipitate production rate (g/h)	Ca mass%	Ca removal rate (g/h)	Mg mass%	Mg removal rate (g/h)
1	122.95	17.56	1.95	0.34	14.7	2.58
2	69.84	10.91	2.58	0.28	16.3	1.78

Table 4-8 presents the XRD analysis results of solid products obtained from the optimised Stage 2 runs using the pre-carbonated magnesium-rich brine from Stage 1. In both runs, the primary product was predominantly nesquehonite, with yields of 89.02 % in Run 1 and 92.70 % in Run 2. This indicates that the Stage 2 process effectively precipitated magnesium selectively from the pre-treated brine with minimal presence of calcium.

Run 1 exhibited a broader range of minor impurities, including silicates, aluminosilicates, and complex calcium compounds. The impact of NaOH dosing on secondary phase formation is also evident. In contrast, Run 2 displayed a simpler impurity profile, primarily composed of monohydrocalcite and anhydrite. This difference highlights the role of NaOH dosing in influencing product composition during Stage 2. The presence of calcium-bearing phases in both runs (*i.e.*, various forms in Run 1 and monohydrocalcite in Run 2) suggests some residual calcium carried over from Stage 1. However, the relatively low amounts indicate effective calcium removal during Stage 1 processing. Overall, the Stage 2 process demonstrates high efficiency in nesquehonite production, with the potential for further optimisation. The results underscore the importance of NaOH dosing management in balancing pH control with minimising impurity formation.

Table 4-8. Stage 2 precipitate XRD speciation results

Mineral	Ideal Chemical Formula	Abundance (%)	
		Run 1	Run 2
Nesquehonite	$Mg(HCO_3)(OH)•_2(H_2O)$	89.02	92.70
Glauberite	$Na_2Ca(SO_4)_2$	0.03	-
Talc	$Mg_3Si_4O_{10}(OH)_2$	2.51	-
Natrolite	$Na_2Al_2Si_3O_{10}•2(H_2O)$	0.72	-
Anorthite	$CaAl_2Si_2O_8$	4.09	-
Apatite	$Ca_5(PO_4)_3F$	1.73	-
Calcite	$CaCO_3$	1.91	-
Monohydrocalcite	$Ca(CO_3)•(H_2O)$	-	5.20
Anhydrite	$Ca(SO_4)$	-	2.10

The experimental mass percentages for magnesium associated with Run 1 (11.52 %) and Run 2 (14.18 %) were lower than for the mass characterisations (at 16.12 % for Run 1 and 16.28 % for Run 2).These results shows that, for Stage 2 precipitates, the trend in experimental data for magnesium content is akin to that of Stage 1, with consistently lower values than those obtained through characterisation. This discrepancy was attributed to ongoing slow reactions occurring in the product vessel during the standing period before filtration.

Table 4-9. Metal balance accountability – Stage 2

Run	Mass precipitate (g)	Element	Mass percentage Experimental (%)	Mass percentage Characterisation (%)	Accountability (%)
1	122.95	Mg	11.52	16.12	60.04
2	69.84	Mg	14.18	16.28	85.15

4.5 MAGNESIUM OXIDE PRODUCT PROTOTYPE

4.5.1 Introduction

Calcination, which is a thermal decomposition process used to convert inorganic materials by removing volatile components, was considered for the synthesis of metal oxides. In the context of magnesium production, this synthesis pathway is typically employed to convert compounds such as $MgCO_3$ into MgO at elevated temperatures. In the case of dolomitic materials, the decomposition occurs in two distinct stages, namely:

$$CaCO_3 \cdot MgCO_3 \rightarrow CaCO_3 \cdot MgO + CO_2 \quad @\ 750\ °C$$

$$CaCO_3 \cdot MgO \rightarrow CaO \cdot MgO + CO_2 \quad @\ 850\ °C$$

The objective of this process step was to further refine the solid product obtained from Stage 2 of the pilot test work, with the aim of producing an MgO prototype product and evaluating the efficiency of the process in yielding a high-purity product. The calcination was performed in a chamber furnace under normal atmospheric pressure at 850 °C—a temperature selected due to the known presence of $CaCO_3$ in the product.

4.5.1.1 Results

The products that were generated from the calcination of materials produced during Stage 2 were analysed for their compositional characteristics. X-ray diffraction analysis results revealed a predominantly MgO-based material (at 83.3 % for Run 1 and 88.2 % for Run 2) with minor impurities (Table 4-10). The primary constituent of the calcined product was periclase (MgO), comprising 81.8 % and 88.2 % of the composition in Run 1 and Run 2, respectively. This increase in MgO content between runs suggests an optimisation of the calcination process. Minor phases identified include portlandite ($Ca[OH]_2$), which decreased from 11.6 % in Run 1 to 6.5 % in Run 2, and calcite ($CaCO_3$), which remained relatively constant at around 5.0 % (Run 1) to 5.5 % (Run 2).

These results demonstrate that the carbonation of magnesium-rich brines followed by calcination can produce a high-purity MgO product. The variation in composition between runs, particularly the increase in periclase content, highlights the potential for process optimisation of the carbonation process to further reduce calcium-based impurities in the Stage 2 product so as to consistently achieve a MgO content that is above 90 % purity.

Table 4-10. MgO product clasification

Compound Name	Ideal formula	Abundance (%)	
		Run 1	Run 2
Nesquehonite	$Mg(HCO_3)(OH)\bullet_2(H_2O)$	1.5	-
Periclase	MgO	81.8	88.2
Portlandite	Ca(OH)2	11.6	6.5
Calcite	$CaCO_3$	5.0	5.5

4.6 FINAL TREATED WATER QUALITY

A significant challenge in maintaining the optimal pH for the process was the need for continuous addition of NaOH. This necessity, while required for pH control, led to a substantial increase in sodium concentrations in the treated water (Table 4-11). The elevated sodium levels, which reached 38 800 mg/ℓ, present a major challenge in the overall treatment process, as no practical methods currently exist for removing sodium from brines on an industrial scale. This limitation substantially affects the feasibility of water reuse or environmental discharge, given that high sodium levels can be harmful to various ecosystems and agricultural applications. Additionally, the treated solution retains a considerable amount of magnesium. This residual magnesium represents a potential resource that could be recovered in additional stages. However, the feasibility of implementing further recovery stages is uncertain due to the overall brine composition. The high sodium content, high sulphate concentrations, as well as the relatively low concentration of remaining magnesium may render additional recovery stages economically unviable.

Table 4-11. Average treated water quality

Concentration (mg/ℓ)								
Na	Al	Ca	Fe	Li	Mg	Mn	Si	Zn
38 800	1.38	19.80	1.80	38.1	589	1.65	52.89	5.65

4.7 CONCLUSION AND RECOMMENDATIONS

The pilot operations consistently achieved high calcium removal rates, with both raw and dosed brine feedstocks demonstrating efficient precipitation of calcium carbonate. This indicates robust repeatability and reliability in the calcium removal process, crucial for CO_2 sequestration efficiency.

While calcium removal showed consistency, magnesium removal exhibited considerable variability. Factors such as competing ion presence, particularly sulphate concentrations, significantly influenced magnesium removal efficiency. The fluctuating patterns underscore the complexity and challenges in maintaining high and consistent magnesium removal rates across different operational conditions.

The study highlights the necessity and effectiveness of a two-stage process for optimising CO_2 sequestration and magnesium recovery from brine. Stage 1 focused on calcium carbonate precipitation, while Stage 2 targeted selective magnesium carbonate precipitation. This study demonstrated improved magnesium removal rates through employing appropriate seeding strategies.

Elevated sulphate concentrations were found to negatively impact magnesium removal efficiency, highlighting the need for careful sulphate management strategies in brine processing to mitigate these effects and enhance overall process efficiency.

The results for solids characterisation with respect to Stage 2 operations and particularly the production of high purity nesquehonite show promising potential for further process optimisation. The consistent production of MgO with minor impurities highlights the feasibility of producing high-value products from brine feedstocks.

In conclusion, the pilot operations demonstrated promising results in terms of calcium removal consistency and the potential for magnesium recovery via a two-stage mineral carbonation process. Future optimisation efforts should focus on addressing variability in magnesium removal and refining process parameters to enhance overall efficiency and product purity.

CHAPTER 5: PREDICTIVE PROCESS MODEL

5.1 INTRODUCTION

This chapter aims to develop a predictive process model to understand the mineral carbonation process more comprehensively. Due to the limitations in testing all possible brine types and conditions experimentally, this model will serve as a crucial simulation tool for predicting various chemical reactions involved in the carbonation process. By exploring different scenarios, the model will allow for a systematic evaluation of the interactions between the different species in the system and help identify optimal conditions for magnesium and calcium removal from brine feedstocks. The carbonation process, as explored in this study, can be represented by a series of chemical reactions (Equations 1 to 14), starting with the equilibrium of species at low concentrations and the instantaneous introduction of CO_2 into the system. The subsequent reactions involving CO_2, water, and the target minerals are described by the relevant equations, which establish a framework for further analysis. Mathematical modelling will be employed to derive dependent differential equations representing the carbonation process. These equations will facilitate the estimation of reaction rates and allow for the evaluation of magnesium and calcium recoveries from brine feedstock with varying mineral content.

The objectives of this chapter are as follows:

1. To constructing a predictive model that encapsulates the key chemical reactions and interactions occurring during mineral carbonation,
2. To test various brine scenarios and ascertain the impacts of different compositions on the carbonation process, given the constraints of experimental testing,
3. To analyse the experimental data from Stage 1 runs and determine reaction rate constants while assessing the model's accuracy against experimental observations, and
4. To evaluate the potential recoveries of magnesium and calcium from increased mineral content brine feedstocks and use the results in completing a techno-economic feasibility study that compares various operational conditions.

By the end of this chapter, a clearer understanding of the carbonation process will be established, along with insights into how different concentrations and brine types impact magnesium and calcium removal efficiencies. This foundational work will pave the way for further exploration of financial viability in treating diverse brine compositions in subsequent chapters.

5.2 PROCESS CHEMICAL REACTIONS

The mineral carbonation process investigated in this study can be represented by reaction R1 to R8 (Mitchell, *et al.*; 2010). Initially, the system was assumed to be at equilibrium, with all species present at low concentrations relative to water. Subsequently, gaseous CO_2 was introduced instantaneously into the system.

$$\mathrm{CO_2(g)} \rightleftharpoons \mathrm{CO_2(aq)} \quad \text{R1}$$

$$\mathrm{CO_2(aq) + H_2O(l)} \rightleftharpoons \mathrm{H_2CO_3(aq)} \quad \text{R2}$$

$$\mathrm{H_2CO_3(aq)} \rightleftharpoons \mathrm{H^+(aq) + HCO_3^-(aq)} \quad \text{R3}$$

$$\mathrm{HCO_3^-(aq)} \rightleftharpoons \mathrm{H^+(aq) + CO_3^{2-}(aq)} \quad \text{R4}$$

$$\mathrm{Ca^{2+}(aq) + CO_3^{2-}(aq)} \rightleftharpoons \mathrm{CaCO_3(s)\downarrow} \quad \text{R5}$$

$$\mathrm{Mg^{2+}(aq) + CO_3^{2-}(aq)} \rightleftharpoons \mathrm{MgCO_3 \cdot 3H_2O(s)\downarrow} \quad \text{R6}$$

$$\mathrm{NaOH(aq)} \rightleftharpoons \mathrm{Na^+(aq) + OH^-(aq)} \quad \text{R7}$$

$$\mathrm{H^+(aq) + OH^-(aq)} \rightleftharpoons \mathrm{H_2O(l)} \quad \text{R8}$$

For Reaction R1, Henry's law provides an estimation of the maximum molar solubility of CO_2 in water, $x_{CO_2(aq,sat)}$, represented by Reaction R9:

$$x_{CO_2(aq,sat)} = k_H p_{CO_2} \quad \text{R9}$$

where:

- $k_H \approx 0.034$ mol/atm (at 25 ºC)
- p_{CO_2} is the partial pressure (in units of atm) at which CO_2 is being injected.

Consequently, the rate equation for R1 can be expressed as:

$$r_{CO_2(g)}|_{R1} = k_1(c_{CO_2(aq)} - c_{CO_2(g)}) \quad \text{R10}$$

assuming that the reaction orders are equal to 1.0. Similarly, the respective rate equations for Reactions R5 and R6 are as follows:

$$r_{Ca^{2+}}|_{R5} = k_5(c_{CaCO_3(sat)} - c_{Ca^{2+}(aq)}) \quad \text{R11}$$

$$r_{Mg^{2+}}|_{R6} = k_6(c_{MgCO_3\cdot 3H_2O(sat)} - c_{Mg^{2+}(aq)}) \quad \text{R12}$$

where $c_{CaCO_3(sat)} \approx 7 \times 10^{-5}$ M and $c_{MgCO_3\cdot 3H_2O(sat)} \approx 9 \times 10^{-3}$ M. Due to the rapid rate at which the intermediary reactions (*i.e.*, R2 – R4) occur, reactions R5 and R6 can be simplified to:

$$Ca^{2+}(aq) + CO_2(aq) + H_2O(l) \rightleftharpoons CaCO_3(s)\downarrow + 2H^+(aq) \quad \text{R13}$$

$$Mg^{2+}(aq) + CO_2(aq) + H_2O(l) \rightleftharpoons MgCO_3(s)\downarrow + 2H^+(aq) \quad \text{R14}$$

5.3 MATHEMATICAL MODELLING

The carbonation process can be described by the following dependant differential equations:

$$\frac{dc_{CO_2(g)}}{dt} = \dot{V}(c_{CO_2(aq)^i} - c_{CO_2(aq)}) + V\left(r_{CO_2(g)}|_{R1} - r_{Ca^{2+}}|_{R5} - r_{Mg^{2+}}|_{R6}\right) \quad \text{R15}$$

$$\frac{dc_{Ca^{2+}(aq)}}{dt} = \dot{V}\left(c_{Ca^{2+}(aq)^i} - c_{Ca^{2+}(aq)}\right) - V \times r_{Ca^{2+}}|_{R5} \quad \text{R16}$$

$$\frac{dc_{Mg^{2+}(aq)}}{dt} = \dot{V}\left(c_{Mg^{2+}(aq)^i} - c_{Mg^{2+}(aq)}\right) - V \times r_{Mg^{2+}}|_{R6} \quad \text{R17}$$

where i represents the concentration of the species at time 0 s, $\dot{V}$ is the volumetric flow rate in ℓ/s, and V is the volume of the reactor in ℓ. The programs and packages used during data-processing and modelling are listed in Table 5-1WinPython 3.9.5 was used to run Python on a Windows® operating system.

Table 5-1. Data-processing and modelling environment information

Scripting language	Python 3.9.5
Data analysis platform	Jupyter Notebook 6.4.0
Packages used	
Pandas	scipy.optimize.minimize
NumPy	scipy.intergrate.solve_ivp

5.4 PREDICTIVE MODEL RESULTS

The experimental data from both Stage 1 runs were independently analysed to fit the reaction rate constants k_1, k_5, k_6. The resulting reaction rates for both runs were found to be similar in magnitude (Table 5-2). The resultant concentration curves of the modelled data, compared to the experimental data are illustrated in Figure 5-1.

Table 5-2. Modelled reaction rate constants

Parameter	Value	Unit
k_1	9.99×10^{-3}	s^{-1}
k_5	8.08×10^{-4}	$M^{-1}s^{-1}$
k_6	1.65×10^{-4}	$M^{-1}s^{-1}$

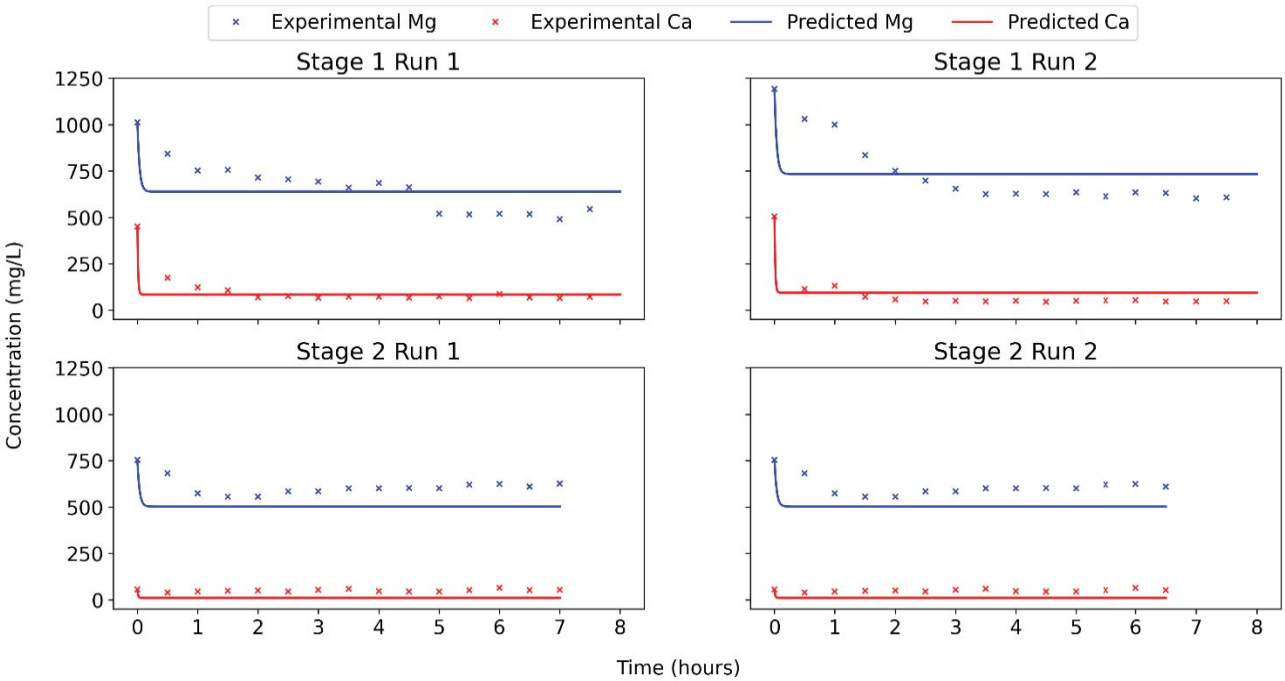

Figure 5-1. Modelled vs experimental concentration curves

The modelled data exhibits a rapid decrease in magnesium and calcium concentrations within the first 10 minutes, contrasting with the experimental data where magnesium shows a slower removal rate and only reaches steady-state removal after 4.5 hours. This disparity suggests complex inhibitory effects, possibly attributable to crystalline growth, which were not accounted for in the predictive model. These disparities could be accounted for by adjusting the reaction order. However, doing so will still not explain the mechanisms associated with these complex inhibitions. Consequentially, although the initial part of the concentration curve could not be accurately predicted, the final concentrations for both Stage 1 runs were reliably estimated, with errors of 21 % for Mg and 15 % for Ca. In Stage 2 runs, promising results were observed with a 17 % error in predicting Mg concentrations. However, due to low Ca concentrations, a large error of 70 % was noted in Stage 2, compounded further when the final experimental value (*i.e.*, 40 mg/ ℓ to 10 mg/ ℓ) was compared to the predictive model.

5.5 THEORETICAL ANALYSIS

The predictive model was employed to determine the recoveries of magnesium and calcium carbonate from a brine feedstock with increased mineral content (Heraldy *et al.,* 2015). This analysis provided essential data on recoveries, which were then used to conduct a techno-economic feasibility study. The objective was to compare the feasibility of the process with higher mineral content, as discussed in Chapter 6.

The concentrations of the feed brine and the subsequent removal of magnesium and calcium in the precipitation stages are listed in Table 5-3. The process was operated as a seven-stage process due to a significant amount of magnesium remaining in the brine after the initial stages.

Figure 5-2 illustrates the removal efficiency and the concentrations of magnesium and calcium across seven consecutive stages of a carbonation process. The removal percentages for both elements exhibit distinct trends throughout the treatment stages.

Calcium removal demonstrates remarkable consistency, maintaining a removal efficiency of approximately 82 % across the first five stages, whereafter a decline was observed as the concentration neared zero. This suggests that the process parameters remain highly favourable for calcium precipitation/removal throughout the entire treatment sequence.

Table 5-3. Increased mineral content brine process predicted removal percentages

Stage	Mg (mg/ℓ)	Ca (mg/ℓ)	Mg removal%	Ca Removal%
Feed	9 010	2 012	-	-
1	4 867	364	46	82
2	2 677	66	45	82
3	1 518	12	43	82
4	906	2.19	40	82
5	582	0.42	36	80
6	410	0.10	29	76
7	320	0.04	22	59

In contrast, magnesium removal shows a gradual decline in efficiency as the process progresses through successive stages. The magnesium removal percentage initiates at approximately 45 % in the first stage and steadily decreases to 22 % at the seventh stage. This declining trend indicates a concentration dependent reduction in the process's effectiveness for magnesium removal.

The concentration curves indicate that after three stages of treatment, nearly all calcium is removed from solution. This is crucial as it suggests that the purity of nesquehonite is significantly enhanced after three stages of treatment. It's important to note that with increased calcium in the feed, multiple stages might be necessary depending on the quality requirements of the final product. Additionally, a substantial amount of magnesium continues to be removed from the solution even after three stages of treatment.

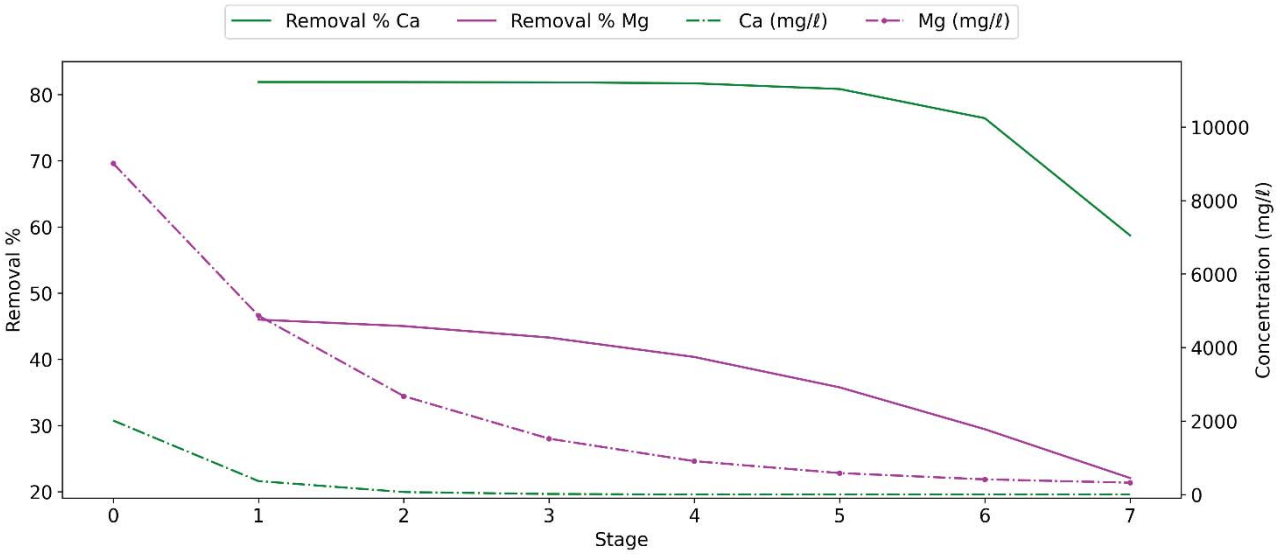

Figure 5-2. Predicted removal% and concentration in mg/ℓ of magnesium and calcium over seven stages treating high mineralised brine

5.6 CONCLUSIONS

The model predictions generally align well with the experimental data, indicating a robust understanding of the carbonation process. These model parameters will be leveraged in the techno-economic assessment of the process for treating brines with varying concentrations, aiming to determine the conditions under which the process can achieve financial viability.

The divergent behaviours of calcium and magnesium removal efficiencies of the highly mineralised feedstock scenario suggest that the underlying mechanisms or process conditions may differentially affect these two elements. The consistently high removal of calcium implies that the process conditions remain optimal for its precipitation or extraction across all stages. However, the decreasing trend in magnesium removal efficiency could be attributed to various factors, including:

- Potential changes in solution chemistry affecting magnesium removal kinetics
- Possible saturation of removal mechanisms specific to magnesium
- Impact of high sulphate concentrations

These results highlight the complexity of multi-element removal in carbonation processes and underscore the need for stage-specific optimisation to maintain high removal efficiencies for both calcium and magnesium throughout the treatment process.

CHAPTER 6: TECHNO ECONOMIC ASSESMENT

6.1 INTRODUCTION

A techno-economic evaluation was conducted using a desktop economic model to assess the feasibility of the process. Capital costs were estimated based on Mintek's *Handbook on the Estimation of Metallurgical Process Costs* by W.T. Ruhmer, with equipment costs updated to current prices using the Chemical Engineering Plant Cost Index (CEPCI). Operating costs and labour expenses were calculated using current market prices for various chemicals, and Mintek's internal labour rates. The market values of the respective minerals and reagents are listed in Table 6-1, along with their sources.

Table 6-1. Costs and market values of reagents and products found in the carbonation process

Mineral	Price (US$/metric ton)	Source
$MgCO_3$	900 – 1500	https://www.made-in-china.com/products-search/hot-china-products/Magnesium_Carbonate_Price.html (accessed 2024-04-28)
$Ca,MgCO_3$ mixed product	100 - 150	https://www.indexbox.io/search/dolomite-market-price/ (accessed 2024-04-28)
MgO	182	https://www.echemi.com/productsInformation/pd20150901228-magnesium-oxide.html (accessed 2024-04-28)
NaOH	300 - 500	www.intratec.us/chemical-markets/caustic-soda-price (accessed 2024-04-28)
CO_2	215 - 373	https://www.chemanalyst.com/Pricing-data/liquid-carbon-dioxide-1090, (accessed 2024-04-28)

The process model was developed using results from optimised pilot operations. To evaluate its feasibility at scale, it was scaled based on the estimated daily brine production of the eMalahleni Water Reclamation Plant (EWRP), which treats 50 Mℓ to 60 Mℓ of acid mine drainage (AMD) per day. Assuming a 60 % water recovery rate, the plant produces approximately 20 Mℓ of brine daily. This scale was chosen to ensure a realistic application of the process.

6.2 FEASIBILITY SCENARIOS

6.2.1 Process flow sheets

To evaluate the feasibility of the process, three process flow sheets were considered as illustrated in Figure 6-1 and Figure 6-2 and Figure 6-3. The first process under examination involves a single-stage approach to generate a calcium and magnesium carbonate complex product of relatively lower value. This strategy, aimed at halving the capital expenditure (Capex) by streamlining the operation into a single stage, is being scrutinised to ascertain its feasibility. The second process being investigated is the two-stage process, where similarly the first stage yields a magnesium and calcium carbonate complex product, while the subsequent stage focuses on producing a high-purity magnesium carbonate product. The third process flowsheet included the use of a calcination step after the Stage 2 process to produce MgO as a final product.

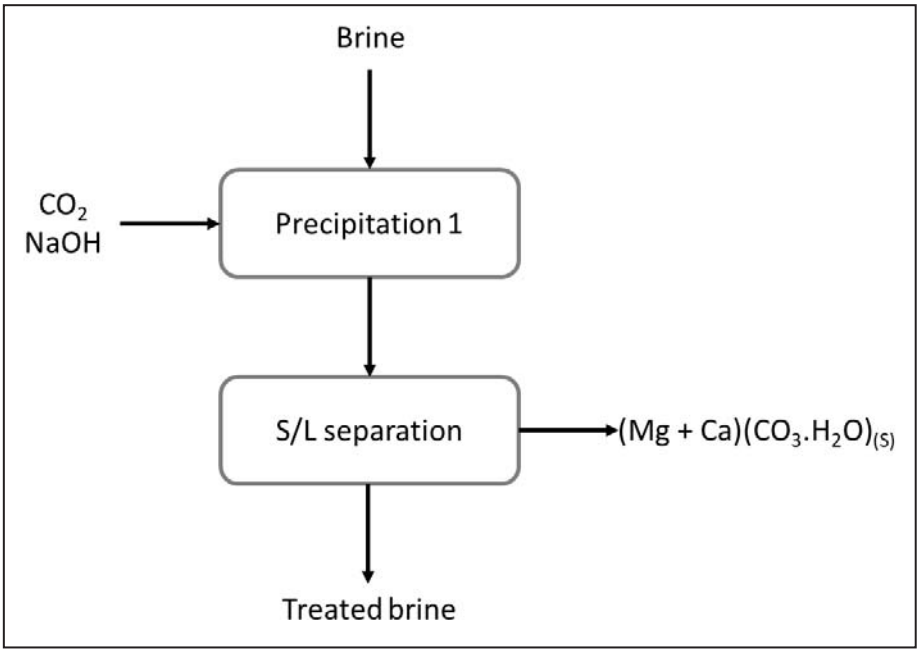

Figure 6-1. Flowsheet 1: One stage treatment process

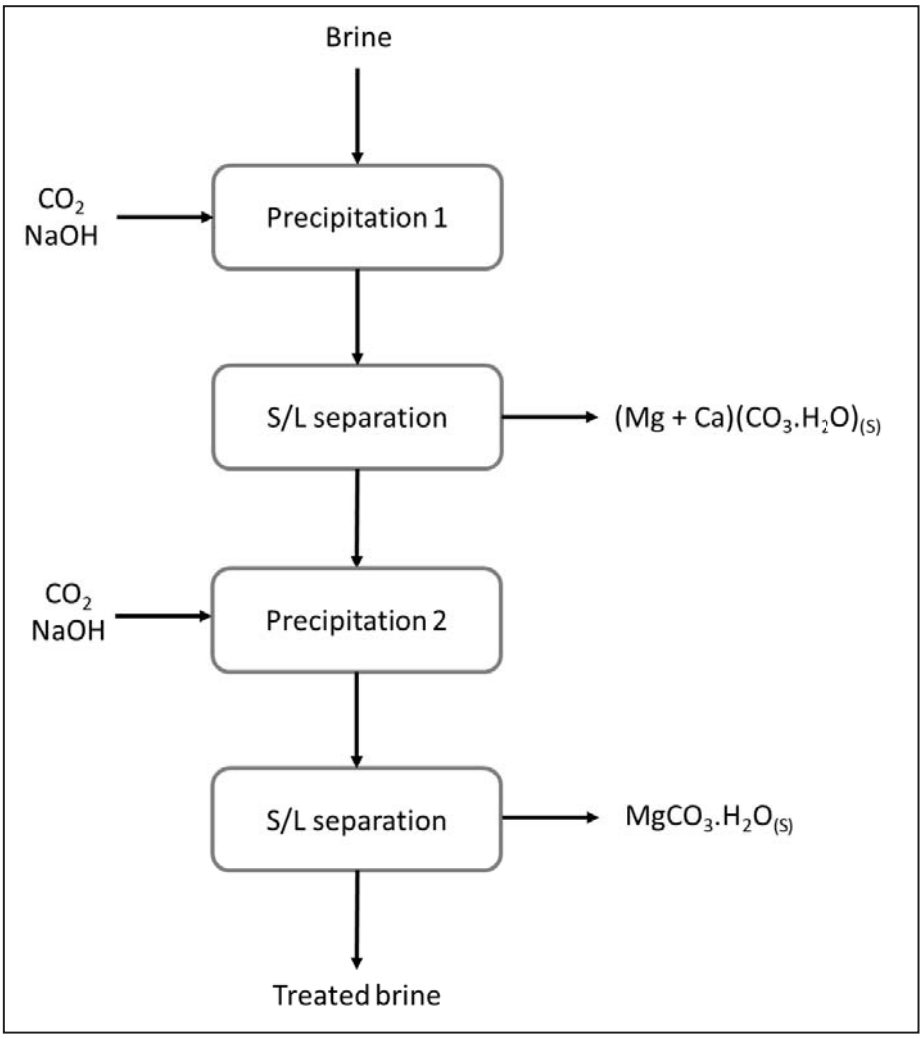

Figure 6-2. Flowsheet 2: Two stage treatment process

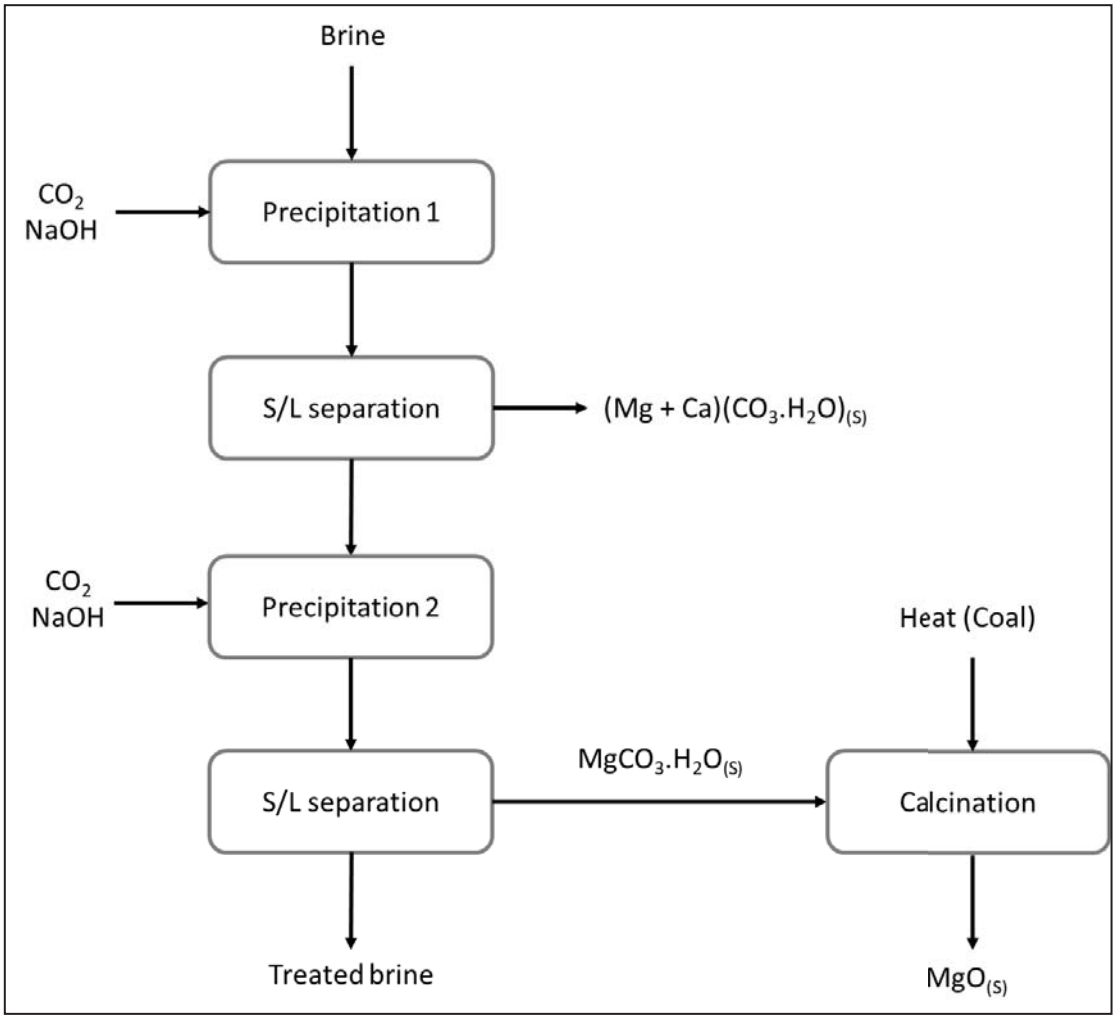

Figure 6-3. Flowsheet 3: Three stage treatment process

6.2.2 Sensitivity investigations

To critically assess the techno-economic feasibility of the process, several key factors were investigated to delineate the conditions under which the treatment of brine, produced from AMD, could be viable. This inquiry involved varying the costs associated with CO_2, considering the utilisation of low-quality or captured CO_2, to discern its potential impact on process profitability. Additionally, the study explored the use of brines with increased mineral concentrations compared to the brine used during piloting, such as those found in seawater desalination reject brine as listed in Table 6-2. The recovery percentages of this brine across both stages were determined using the predictive model developed in Chapter 5. The equipment proposed for the Capex evaluation for each of the cases described in this chapter are presented in APPENDIX C: Techno economic investigation parameters.

Table 6-2. Brine compositions modelled

Brine type	Mg (mg/ℓ)	Ca(mg/ℓ)	Source
Experimental brine	1 200	400	-
Seawater reject brine	9 010	2 012	Heraldy *et al.*,2015

6.2.2.1 Flowsheet 1 – One stage treatment process

The scenarios investigated for Flowsheet 1 configuration are outlined in Table 6-3.

Table 6-3. Economic feasibility scenarios investigated for Flowsheet 1 configuration

Case	Case description
1.1	Study derived from pilot-scale findings for a single stage process
1.2	Analysis incorporating (80 % - 100 %) reduced CO_2 expenses
1.3	Investigation exploring elevated mineral concentrations (Ca and Mg) as listed in Table 6-2
1.4	Investigation exploring elevated mineral concentrations (with (80 % - 100 %) reduced CO_2 costs)

6.2.2.2 Flowsheet 2 – Two stage treatment process

The scenarios investigated for Flowsheet 1 configuration are outlined in Table 6-4. The first case explores findings derived from pilot-scale operations, which investigats economic feasibility based on scaled-up operational insights. The second case incorporates an analysis that considers a substantial reduction (*i.e.*, 80 % - 100 %) in CO_2 expenses. This investigation seeks to evaluate the process's viability under reduced operational costs, aiming to determine potential cost-effectiveness and economic benefits. The last two cases investigate the utilisation of brines with elevated mineral concentrations, as specified in Table 6-2. These scenarios explore how these higher concentrations affect process efficiency and economic feasibility and aim to identify optimal conditions for resource recovery and commercial viability.

Table 6-4. Economic feasibility scenarios investigated for Flowsheet 2 configuration

Case	Case description
2.1	Study derived from pilot-scale findings for a two-stage process
2.2	Analysis incorporating (80 % - 100 %) reduced CO_2 expenses for investigation
2.3	Investigation exploring elevated mineral concentrations as listed in Table 6-2
2.4	Investigation exploring elevated mineral concentrations as listed in Table 6-2, including a third precipitation step where additional product is recovered from solution

6.2.2.3 Flowsheet 3 – Three stage treatment process

The scenarios investigated for Flowsheet 3 configuration are outlined in Table 6-5.

Table 6-5. Economic feasibility scenario investigated for Flowsheet 3 configuration

Case	Case description
3.1	Study derived from pilot-scale findings for a three-stage process
3.2	Investigation exploring elevated mineral concentrations as listed in Table 6-2

6.3 ECONOMICS FEASIBILITY INVESTIGATION

The findings from the techno-economic analysis are summarised in sections below providing insights into the revenue, operational costs, and Capex associated with each investigated case.

6.3.1 Flowsheet 1 – One stage treatment process

The results of the economic assessment of Flowsheet 1's process configuration is summarised in Table 6-6. For the single-stage process, represented by Cases 1.1 (baseline) and Case 1.2 (80 % and 100 % CO_2 cost reduction), it becomes evident that even with reduced CO_2 costs, the current water quality renders the process financially unfeasible. Revenue accounts for a mere 10 % of operational costs. This disparity persists even with increased mineral concentration in Cases 1.3 and Case 1.4 (80 % and 100 % CO_2 cost reduction), where the maximum revenue-to-Opex ratio reaches only 90 %, excluding CO_2 costs. Consequently, the one-stage process proves unprofitable, as it yields a low-value mixed product primarily suitable for fertiliser applications.

Table 6-6. Flowsheet 1: economic feasibility investigation results

Case	Revenue (million US$/annum)	Opex (million US$/annum)	Capex (million $)
1.1	5.99	51.71	25.43
1.2	6.24	$50.50^{80\ \%}$ $45.70^{100\ \%}$	25.43
1.3	41.51	51.72	25.86
1.4	41.51	$52.84^{80\ \%}$ $47.33^{100\ \%}$	25.86

To gain a deeper understanding of the limitations and primary drivers of operational expenditure (Opex), Case 1.3 was analysed in detail. Due to its higher mineral content, Case 1.3 demonstrated the greatest potential for success compared to scenarios with lower mineral concentrations, as illustrated in Table 6-7. The analysis revealed that NaOH is the predominant contributor to operating expenses, accounting for 84 % of the total costs. This finding underscores the critical role of NaOH in the process, making it a pivotal factor for the overall success of the operation.

Table 6-7. Flowsheet 1: Opex outline Case 1.3

Outline	Case 1.3	
	Million US$	%
Labour	1.18	2.28
NaOH	43.51	84.13
CO_2	6.01	11.62
Power	0.26	0.50
Maintenance	0.75	1.46

6.3.2 Flowsheet 2 – Two stage treatment process

The results of the economic assessment of Flowsheet 2's process configuration is summarised in Table 6-8. For the baseline two-stage process, evaluated in Case 2.1, demonstrates revenue accounting for just 15 % of the Opex. Despite a slight reduction in operational costs with reduced CO_2 expenses, the process remains economically infeasible given the prevailing water quality conditions.

Exploring scenarios involving increased mineral content, Case 2.3 demonstrates revenue exceeding 190 % of the Opex costs without CO_2 cost reductions. This heightened mineral content in the target brine solution results in an internal rate of return (IRR) of 27.3 %, indicating a favourable return on investment. When adding an additional recovery step, as in Case 2.4, the revenue increases but the ratio between the Opex and total revenue decreases to 160 %, along with a reduction of the IRR to 17.9 %.

Table 6-8. Flowsheet 2: economic feasibility investigation results

Case	Revenue (million $/annum)	Opex (million $/annum)	Capex (million $)
2.1	14.06	91.32	57.77
2.2	14.06	$88.51^{80\ \%}$ $77.29^{100\ \%}$	57.77
2.3	175.29	92.48	93.83
2.4	245.96	153.76	163.06

Finding high magnesium concentrations in RO brines from AMD treatment poses significant challenges. RO brines typically have lower magnesium concentrations, and increasing these levels to the necessary threshold is difficult due to the limitations of the AMD treatment process and the variability in feed water composition. Therefore, optimisation of both the removal efficiency and feed water mineral content is crucial to enhancing the feasibility of this process.

6.3.3 Flowsheet 3 – Three stage treatment process

The economic evaluation of Flowsheet 3's process configurations, as summarised in Table 6-9, shows that for Case 3.1, a considerable decrease in revenue occurs compared to Case 2.1, primarily attributed to the diminished value of MgO in contrast to $MgCO_3$. This difference poses a significant challenge as it not only lowers the product's market value but also compromises CO_2 sequestration efforts by reintroducing captured CO_2 into the environment. Furthermore, Case 3.2 demonstrates that despite using feedstock with significantly increased mineral content, the fundamental issue with Flowsheet performance lies in the economic dynamics of MgO pricing. This highlights a more favourable prospect for producing the $MgCO_3$ precursor, as achieved in Flowsheet 2.

Table 6-9. Flowsheet 3: economic feasibility investigation results

Case	Revenue (million $/annum)	Opex (million $/annum)	Capex (million $)
3.1	7.18	107.62	82.78
3.2	46.01	132.24	236.48

6.4 CONCLUSIONS AND RECOMMENDATIONS

In conclusion, the economic feasibility analysis highlighted the significant challenges associated with the proposed processes. It was determined that the process must function as a two-stage system that produces primarily carbonates as products. This is due to the low-value of mixed $CaMgCO_3$ product produced in a single-stage process, and the low market value of MgO (compared to $MgCO_3$), which is produced in a three-stage process where the CO_2 sequestered is re-released into the environment via calcination.

The primary limiting factors for the financial feasibility of the two-stage process are:

1. The availability of adequate mineral concentrations in the feed water, and
2. The ability to achieve high magnesium recovery rates in the second stage of the process.

Exploring scenarios involving increased mineral content, such as in Cases 2.3 and 2.4, demonstrates that higher mineral content in the feed water significantly enhances economic feasibility. For instance, Case 2.3 shows an IRR of 27.3 % with revenue exceeding 190 % of Opex costs, while Case 2.4, despite higher revenue, realises a reduction in IRR due to increased costs. This suggests that while the additional recovery stages may improve gross revenue, they also introduce higher costs that outweigh the benefits in terms of the rate of return.

The major driver of operational costs is NaOH, which constitutes to at least 80 % of the Opex. If a substitute alkali is utilised instead (ideally magnesium hydroxide [$Mg(OH)_2$], with a focus on magnesium recovery), costs could be significantly reduced due to the potential recovery of the calcium and magnesium from the hydroxide chemicals for pH control in the products.

CHAPTER 7: CONCLUSIONS & RECOMMENDATIONS

7.1 CONCLUSIONS

Several key conclusions can be drawn from the piloting of the two-stage mineral carbonation process for CO_2 sequestration and valuable product recovery from brine. The study demonstrated the technical feasibility of the process, achieving high calcium removal rates and improved magnesium removal through optimised seeding strategies in the second stage. The production of high-purity nesquehonite (of around 89 % to 93 %) in Stage 2 and subsequent calcination to high-purity MgO (of 81.8 5 to 88.2 % periclase) highlights the potential for generating valuable products.

The economic viability of the process is heavily dependent on the mineral content of the feed brine. The techno-economic assessment indicated that the process was financially viable when treating high mineral content brines, with potential revenue exceeding 147 % of operational expenses and an internal rate of return of 15.4 %. Although additional recovery stages may improve gross revenue, they may also introduce higher costs that outweigh the benefits in terms of the rate of return. However, the process faces significant economic challenges due to high operational costs, predominantly driven by NaOH consumption for pH control, which accounts for approximately 84 % of the total operational expenses.

From an environmental perspective, the process effectively sequesters CO_2 but produces sodium-rich treated water that poses its own challenges with respect to disposal or reuse. Additionally, elevated sulphate concentrations negatively impact magnesium removal efficiency and present a significant technical hurdle that requires further investigation and mitigation strategies.

The developed predictive model demonstrates good alignment with experimental data, particularly in estimating final concentrations, providing a valuable tool for process optimisation and scale-up considerations. However, its limitations in capturing initial kinetics suggest complex inhibitory effects warrant further investigation.

7.2 RECOMMENDATIONS

Firstly, future research should focus on optimising the process for high mineral content brines, such as those from seawater desalination, to maximise economic potential. Concurrently, investigation into alternative pH control methods, particularly in the use of magnesium hydroxide, could significantly reduce operational costs due to the recovery of the neutralising agent in the product, without loading sodium into the treated brine, which is already difficult to remediate as is.

Secondly, further process optimisation efforts should target improved magnesium removal rates and consistency, with a specific emphasis on developing strategies to mitigate the adverse effects of high sulphate concentrations. Exploration of low-cost or captured CO_2 sources could further enhance the economic viability of the process and to assess the impacts of pollutants on the purity of the produced products. Additionally, conducting larger-scale pilot studies using high mineral content brines is crucial to validate economic projections and process performance at the industrial scale.

Lastly, from an environmental perspective, a comprehensive lifecycle assessment is recommended to quantify the net environmental benefits, including CO_2 sequestration potential and the implications of treated water management. This assessment should inform the development of integrated solutions for brine treatment and CO_2 sequestration within broader water management and climate mitigation strategies.

REFERENCES

Abdul-Wahab, S.A. & Al-Weshahi, M.A. (2009). Brine management: substituting chlorine with on-site produced sodium hypochlorite for environmentally improved desalination processes. *Water Resources Management*, 23, pp. 2437-2454.

Akcil, A. & Koldas, S. (2006). Acid mine drainage (AMD): causes, treatment and case studies. *Journal of Cleaner Production*, 14, pp. 1139-1145.

Bai, H., Kang, Y., Quan, H., Han, Y., Sun, J. & Feng, Y. (2013). Treatment of acid mine drainage by sulphate-reducing bacteria with iron in bench scale runs. *Bioresource Technology*, 128, pp. 818-822.

Centre for Environmental Rights (2024). Acid mine drainage. Available at: https://cer.org.za/programmes/mining/environmental-issues/acid-mine-drainage [Accessed 05 Aug. 2024].

Choi, K.W., Ahn, Y., Kang, C.U., Chon, C.M., Prabhu, S.M., Kim, D.H., Ha, Y.H. & Jeon, B.H. (2023). Morphology and stability of mineralized carbon influenced by magnesium ions. *Environmental Science and Pollution Research*, 30(16), pp. 48157-48167.

CSIR (2009). Acid mine drainage in South Africa. Briefing Note.

Cunha, M.P., Ferraz, R.M., Sancinetti, G.P. & Rodriguez, R.P. (2019). Long-term performance of a UASB reactor treating acid mine drainage: effects of sulphate loading rate, hydraulic retention time, and COD/SO4^2− ratio. *Biodegradation*, 30, pp. 47-58.

Dananjayan, R., Kandasamy, P. & Andimuthu, R. (2016). “Direct mineral carbonation of coal fly ash for CO_2 sequestration”, Journal of Cleaner Production, 112:4173-4182. https://doi.org/10.1016/j.jclepro.2015.05.145.

Dhir, B. (2018). Biotechnological tools for remediation of acid mine drainage (removal of metals from wastewater and leachate). In: M.N.V. Prasad, P.J. De Campos Favas & S.K. Maiti, (eds.). *Bio-Geotechnologies for Mine Site Rehabilitation*. Elsevier, Amsterdam, pp. 67-82.

du Preez, K. (2021). Mintek’s integrated cloSURETM technology for treatment of acid mine drainage. In: *International Mine Water Association Conference Proceedings 2021 – Mine Water Management for Future Generations*.

Fundikwa, B. (2019). Using groundwater: options for managing saline wastewater/brine. *GreenCape*, Industry brief.

Fagerlund J, Nduagu E, Romão I, Zevenhoven R. (2010). A stepwise process for carbon dioxide sequestration using magnesium silicates. Front. Chem. Eng. China, , 4: 133-41

Galvez-Martos, J., Elhoweris, A., Morrison, J. & Al-Hor, R., Y. (2018). “Conceptual design of a CO2 capture and utilisation process based on calcium and magnesium rich brines”. Journal of CO_2 Utilization, 27:161-169. DOI: 10.1016/j.jcou.2018.07.011.

Heraldy, E., Santosa, S.J., Triyono, W. & Wijaya, K. (2015). Anionic and cationic dyes removal from aqueous solutions by adsorption onto synthetic Mg/Al hydrotalcite-like compounds. *Indonesian Journal of Chemistry*, 15(3), pp. 234-241.

International Energy Agency (IEA) (2022). CO2 emissions in 2022. Available at: https://www.iea.org/reports/co2-emissions-in-2022 [Accessed 06 Aug. 2024].

International Energy Agency (IEA) (2024). How much CO2 does South Africa emit? Available at: https://www.iea.org/countries/south-africa/emissions [Accessed 06 Aug. 2024].

International Energy Agency (IEA) (2023). Carbon capture utilisation and storage. Available at: https://www.iea.org/energy-system/carbon-capture-utilisation-and-storage.

Ji, L., Yu, H., Wang, X., Grigore, M., French, D., Gozukara, Y., Yu, J. & Zeng, M. (2017). "CO2 sequestration by direct mineralisation using fly ash from Chinese Shenfu coal". Fuel Process Technology, 156:429-437. https://doi.org/10.1016/j.fuproc.2016.10.004.

Lattemann, S. & Höpner, T. (2008). Environmental impact and impact assessment of seawater desalination. *Desalination*, 220, pp. 1-15.

McCarthy, S.T. (2011). The impact of acid mine drainage in South Africa. *South African Journal of Science*, 107.

McLaughlin, H., Littlefield, A.A., Menefee, M., Kinzer, A., Hull, T., Sovacool, B.K., Bazilian, M.D., Kim, J. & Griffiths, S. (2024). Carbon capture utilization and storage in review: sociotechnical implications for a carbon reliant world. *Renewable and Sustainable Energy Reviews*, 177, 113215. Available at: https://doi.org/10.1016/j.rser.2023.113215.

Mezher, T., Fath, H., Abbas, Z. & Khaled, A. (2010). Techno-economic assessment and environmental impacts of desalination technologies. *Desalination*, 266, pp. 263-273.

Miri, R. & Chouikhi, A. (2005). Ecotoxicological marine impacts from seawater desalination plants. *Desalination*, 182, pp. 403-410.

Mitchell, M.J., Jensen, O.E., Cliffe, K.A. & Maroto-Valer, M.M. (2010). A model of carbon dioxide dissolution and mineral carbonation kinetics. *Proceedings of the Royal Society A: Mathematical, Physical and Engineering Sciences*, 466(2117), pp. 1265-1290.

Naidoo, Y. (2013). "A Study into the viability of Mineral Carbonation as a means of CO2 sequestration in South Africa", Master's Thesis, University of the Witwatersrand, South Africa. http://hdl.handle.net10539/13496

Nyambura, M.G., Mugera, G.W., Felicia, P.L. & Gathura, N.P. (2011). Carbonation of brine impacted fractionated coal fly ash: implications for CO2 sequestration. *Journal of Environmental Management*, 92(3), pp. 655-664.

Olajire, A.A. (2013). A review of mineral carbonation technology in sequestration of CO2. *Journal of Petroleum Science and Engineering*, 109, pp. 364-392.

Siriruang, C., Toochinda, P., Julnipitawong, P. & Tangtermsirikul, S. (2017). "CO2 capture using fly ash from coal fired power plant and applications of CO2-captured fly ash as a mineral admixture for concrete", Journal of Environmental Management, 170:70-78. DOI: 10.1016/j.jenvman.2016.01.010.

Wu, H., Huang, Q., Xu, Z., Sipra, A.T., Gao, N., Vandenberghe, L.P.S., Vieira, S., Soccol, C.R., Zhao, R., Deng, S., Boetcher, S.K.S., Lu, S., Shi, H., Zhao, D., Zhang, Y., Hu, G., Webley, P.A., Liang, D., Ba, Z., Mlonka-Mędrala, A., Magdziarz, A., Miskolczi, N., Tomasek, S., Lam, S.S., Foong, S.Y., Ng, H.S., Jiang, L., Yan, X., Liu, Y., Ji, Y., Sun, H., Zhang, Y., Yang, H., Zhang, X., Sun, M., Tsang, D.C.W., Shang, J., Müller, C., Rekhtina, M., Krödel, M., Bork, A.H., Donat, F., Liu, L., Jin, X., Liu, W., Saqline, S., Wu, X., Xu, Y., Khan, A.L. & Ali, Z. (2024). A comprehensive review of carbon capture science and technologies. *Carbon Capture Science & Technology*, 11, 100178. Available at: https://doi.org/10.1016/j.ccst.2023.100178.

APPENDIX A: Raw data

A1.1 – Laboratory scale optimisation data

Stage 1 CO_2 optimisation			Stage 2 CO_2 optimisation		
Time (h)	Ca (mg/ℓ)	Mg (mg/ℓ)	Time (h)	Mg (mg/ℓ)	Ca (mg/ℓ)
0	450.0069	980.02	0	1068.10	121.81
0.5	405.91	911.36	0.5	961.83	77.42
1	293.19	904.61	1	822.95	68.48
1.5	-	870.38	1.5	796.76	60.37
2	186.12	843.66	2	753.42	55.21
2.5	248.63	898.62	2.5	812.22	34.31
3	175.08	873.37	3	723.29	34.62
3.5	-	879.96	3.5	914.27	59.09
4	-	914.40	4	713.74	17.46
4.5	38.58	864.99	4.5	772.07	97.10
5	50.47	869.44	5	750.21	59.02
5.5	100.54	896.02	5.5	771.42	104.08
6	163.46	912.96	6	826.97	44.60

A1.2 – HRT optimisation data Stage 1

HRT 2 ℓ/h			HRT 3 ℓ/h			HRT 4 ℓ/h		
Time (h)	Mg (mg/ℓ)	Ca (mg/ℓ)	Time (h)	Mg (mg/ℓ)	Ca (mg/ℓ)	Time (h)	Mg (mg/ℓ)	Ca (mg/ℓ)
0	1219.32	334.41	0	1250.70	501.85	0	1262.49	356.36
0.5	1176.80	181.73	0.5	963.06	267.00	0.5	918.01	251.88
1	1147.47	148.34	1	975.70	98.13	1	1103.20	237.40
1.5	1104.33	98.73	1.5	911.60	37.35	1.5	1060.27	89.68
2	1166.76	159.45	2	980.93	47.56	2	1122.99	97.98
2.5	1110.21	97.47	2.5	1040.02	54.31	2.5	1106.15	89.70
3	1115.84	67.49	3	1072.80	28.48	3	1115.18	89.23
3.5	1139.68	54.66	3.5	1104.69	53.09	3.5	1140.24	109.55
4	1115.42	58.90	4	1103.99	42.29	4	1106.90	115.94
4.5	1145.50	86.83	4.5	1004.04	49.78	4.5	1060.59	113.96
			5	1015.77	0.00	5	1195.64	148.93
			5.5	1084.08	94.75	5.5	1169.87	160.03
			6	1140.64	111.07	6	1123.25	160.64
			6.5	1155.54	117.19			

A1.2 – HRT optimisation Stage 2

HRT 2 ℓ/h		HRT 3 ℓ/h		HRT 4 ℓ/h	
Time (h)	Mg (mg/ℓ)	Time (h)	Mg (mg/ℓ)	Time (h)	Mg (mg/ℓ)
0	1070.95	0	1372.77	0	1068.10
0.5	1060.42	0.5	1029.22	0.5	961.83
1	922.60	1	972.51	1	822.95
1.5	815.20	1.5	985.14	1.5	796.76
2	790.02	2	797.82	2	753.42
2.5	690.53	2.5	891.99	2.5	812.22
3	811.97	3	885.30	3	723.29
3.5	739.46	3.5	882.33		
4	787.94	4	958.02		
4.5	726.21	4.5	953.97		
5	737.88	5	953.97		

A2.1 - Baseline pilot runs Stage 1`

	Raw		Dosed	
Time (h)	Ca (mg/ℓ)	Mg (mg/ℓ)	Ca (mg/ℓ)	Mg (mg/ℓ)
0	299.02	276.77	333.74	1233.74
0.5	242.27	231.77	186.91	1169.13
1	289.28	226.01	32.38	1139.88
1.5	207.55	209.52	11.22	1088.01
2	121.44	150.14	86.97	786.97
2.5	0.00	194.35	33.15	733.15
3	0.00	252.21	75.88	872.35
3.5	0.00	164.94	70.00	890.96
4	0.00	223.95	12.98	716.60
4.5	0.00	171.92	95.53	695.53
5	0.00	262.93		

A2.2. Base pilot runs – Stage 2 data

	Raw		Dosed	
Time (h)	Ca (mg/ℓ)	Mg (mg/ℓ)	Ca (mg/ℓ)	Mg (mg/ℓ)
0	118.25	218.83	37.44	733.41
0.5	92.34	190.72	30.00	641.34
1	53.50	190.43	93.01	638.59
1.5	15.73	184.58	91.36	649.66
2	1.93	168.58	42.30	642.47
2.5	0.00	160.63	28.54	628.54
3	0.00	160.03	44.33	648.41
3.5	0.00	143.88	23.12	526.82
4	0.00	148.16	81.90	583.26
4.5	0.00	148.71	80.76	560.98

A3.1 Optimised pilot run 1

	Stage 1 run 1		Stage 2 run 1	
Time (h)	Ca (mg/ℓ)	Mg (mg/ℓ)	Ca (mg/ℓ)	Mg (mg/ℓ)
0	450.24	1013.32	54.88	754.68
0.5	175.09	842.65	39.45	681.46
1	122.57	751.99	45.57	573.17
1.5	107.04	755.49	47.80	555.20
2	69.38	714.64	49.71	555.51
2.5	76.51	705.66	44.95	584.39
3	67.12	693.85	53.99	583.50
3.5	72.05	661.28	58.93	600.97
4	71.23	685.95	47.05	599.78
4.5	66.36	662.53	45.22	602.90
5	73.94	520.13	44.82	600.92
5.5	65.04	516.39	51.93	620.71
6	86.33	519.30	64.05	624.77
6.5	67.66	517.44	51.87	610.53
7	65.07	491.45	54.40	625.05
7.5	72.28	544.31		

A3.2 Optimised pilot run 2

	Stage 1 run 2		Stage 2 run 2	
Time (h)	Ca (mg/ℓ)	Mg (mg/ℓ)	Ca (mg/ℓ)	Mg (mg/ℓ)
0	45.57	1192.50	0.48	665.00
0.5	113.48	1031.20	3.26	508.75
1	131.08	999.51	14.74	545.62
1.5	72.25	835.48	17.10	500.48
2	56.98	751.25	13.71	530.47
2.5	46.49	698.36	11.25	506.99
3	50.28	654.93	16.45	545.92
3.5	45.96	625.75	11.94	536.52
4	50.58	627.75	12.92	560.62
4.5	45.58	625.37	8.61	569.59
5	50.52	635.08	9.26	570.30
5.5	51.47	613.39	16.15	566.63
6	54.50	635.54	6.67	568.13
6.5	47.23	631.79	4.74	606.78
7	46.69	602.12		
7.5	48.34	608.64		
8	46.74	603.40		

APPENDIX B: Predictive model code

```
import numpy as np
import matplotlib.pyplot as plt
import scipy as sp
from scipy.integrate import solve_ivp
import pandas as pd
from scipy.optimize import minimize
import math
from scipy.interpolate import interp1d
from scipy.optimize import curve_fit

# Experimental data
df = pd.read_excel('Data.xlsx', sheet_name='Sheet1')

# Stage 1 Run 1
df.dropna(subset=['Time (s) 11', 'Mg mol 11', 'Ca mol 11', 'Time (h) 11'],
inplace=True)

Time_exp_1_1 = df['Time (s) 11']
Mg_exp_1_1 = df['Mg mol 11']
Ca_exp_1_1 = df['Ca mol 11']
Timex_1_1 = df['Time (h) 11']

Ca_plat_1_1 = df['Plat Ca 11'].iloc[0]
Mg_plat_1_1 = df['Plat Mg 11'].iloc[0]

# Last time vale h
Timex_1_1_array = Timex_1_1.values
Timed_1_1 = Timex_1_1_array[-1]

# Last time vale s
Time_1_1_array = Time_exp_1_1.values
Timesd_1_1 = Time_1_1_array[-1]

# Initial concs
Ca0_1_1 = Ca_exp_1_1.iloc[0]
Mg0_1_1 = Mg_exp_1_1.iloc[0]

# FLow rate
Q_h = 15.1 # L/h
v = Q_h/3600 #L/s
V = 22.7 # L
tau = V/v #residence time in s

CO2vhour = 42.6 #L/h
CO2v = 2.15 # mol/s
CO2g0 = 0

# CO2 saturation calc
kh = 0.034 # mol/atm
Pco2 = 4.5*0.25 # atm
```

```
Pco2atm = 1
CO2aq0 = kh*Pco2atm
CO2aqsat = kh*Pco2#mol

S_0_1_1 = (CO2g0,CO2aq0, Ca0_1_1, Mg0_1_1)
#k guess
k1_init = 1e-2
k5_init = 5e-4
k6_init = 2e-1

Ca_sat = 7e-5
Mg_sat = 9e-3

def fit_k_1_1(params):
  k1, k5, k6_max, alpha, beta= params
  def dSdx(x, S):
    CO2g, CO2aq, Ca, Mg = S
    k6 = k6_max * (1 - np.exp(-alpha * (x - beta)))
    r1 = k1*(CO2aqsat - np.max([0,CO2aq]))
    epsilon = 1e-10
    r5          =          k5*(np.max([0,Ca])-Ca_sat)*(np.max([0,CO2aq])          +
epsilon)**0.0001#*induction_factor#
    r6 = k6*(np.max([0,Mg])-Mg_sat)*(np.max([0,CO2aq])+ epsilon)**0.0001

    return [CO2v-r1*V,
        CO2aq0*v-np.max([0,CO2aq])*v + (r1 - r5 - r6)*V,
        np.max([0,Ca0_1_1])*v - np.max([0,Ca])*v + (-r5)*V,
        np.max([0,Mg0_1_1])*v - np.max([0,Mg])*v + (-r6)*V]

  t_eval = np.linspace(0,Timesd_1_1, 16)
  sol  =  solve_ivp(dSdx,  (0,  Timesd_1_1),  y0=S_0_1_1,  method='BDF',  t_eval  =
t_eval, rtol=1e-10, atol=1e-10) #BDF
  t = sol.t
  Ca_pred = sol.y[2]#*(Ca_mw*1000)
  Mg_pred = sol.y[3]#*(Mg_mw*1000)

   # Calculate error function
  error = np.sum((Mg_pred - Mg_exp_1_1)**2)+ np.sum((Ca_pred - Ca_exp_1_1)**2)
  return error

bounds = [(0.0,0.2),(0.0, 1), (0.0, 0.0002), (0.0, 100), (0.0, Timesd_1_2/2)]
res_1_1 = minimize(fit_k_1_1, [k1_init, k5_init, k6_init, 0.1, Timesd_1_2/10],
method="SLSQP", bounds=bounds, tol=1e-12)

# Assaign conc
Ca_pred_1_1 = sol_1_1.y[2]
Mg_pred_1_1 = sol_1_1.y[3]
Time_pred_1_1 = sol_1_1.t
CO2aq_pred_1_1 = sol_1_1.y[1]
CO2g_pred_1_1 = sol_1_1.y[0]
```

APPENDIX C: Techno economic investigation parameters

Table C-1. Labour force for a plant treating 20 Mℓ/day

Position	$/annum	Quantity	Total $/annum	Basis
Metallurgical				
Production Superintendent	55,000	1	55,000	BioCop '95 $20000, Fenix '06 $79042, Penoles '02 $36384
Plant Metallurgist	60,000	1	60,000	BioCop '95 $15000, Fenix '06 $60801, Penoles '02 $27300, Wardrop '07 $90000
Process Engineer	50,000	1	50,000	Fenix '06 $46770 Penoles '02 $18456
Metallurgical Technician	60,000	2	120,000	Fenix '06 $27675 Penoles '02 $9180
Chief Chemist	50,000	1	50,000	Fenix '06 $60801, Penoles '02 $18456
Shift Chemist	20,000	3	60,000	Fenix '06 $27675, Penoles '02 $9180
Sample preparers	15,000	10	150,000	Fenix '06 $9690, Penoles '02 $5952
Department Secretary/Clerk	15,000	2	30,000	
Operations				
Precipitation 1	30,000	10	300,000	BioCop '95 R73000, Fenix '06 $16376, Penoles '02 $9180, Wardrop '07 $55000
Precipitation 2	30,000	10	300,000	
Calcination	30,000	10	300,000	
Shift foreman	35,000	1	35,000	BioCop '95 R150000, Fenix '06 $35977, Penoles '02 $10692
Day Operators (shift coverage)	15,000	15	225,000	Fenix '06 $9690, Penoles '02 $5952
Department Secretary/Clerk	15,000	2	30,000	
Maintenance				
Maintenance superintendent	80,000	2	160,000	Fenix '06 $79042, Penoles '02 $36384
Maintenance engineers	70,000	2	140,000	Fenix '06 $60801, Penoles '02 $27300
Maintenance planners	40,000	2	80,000	
Maintenance foreman	30,000	2	60,000	
Electrician/Instrument fitter	30,000	4	120,000	
Fitter	30,000	4	120,000	Fenix '06 $35977, Penoles '02 $10692
Boiler maker / welder	30,000	4	120,000	
Other trades (crane/machinist etc)	30,000	2	60,000	
Apprentices	15,000	10	150,000	Fenix '06 $9690, Penoles '02 $5952
Department Secretary/Clerk	15,000	2	30,000	
		Total labour	**2,805,000**	**$/annum**

Item	size					a	b	c	Cost	Cost
	smallest	largest	used	used					R('000)	R('000)
Precipitation 1	Min	Max	Used			a	b	c	Cost/unit	USD 14,893,008
Reaction tanks	1.0	21.0	1792.23	m^3	86.0	3.00E+03	2.88E+03		11,229	USD 965,722
Reacion tanks agitator	5.0	400.0	1792.23	m^3	5.0	7.22E+00	2.23E-01	-9.326E-05	20,522	USD 102,608
Feed pump	1.4	27.2	833.33	m^3/h	31.0	1.13E+05	3.77E-01		15553	USD 482,150
Feed tank	1.0	21.0	1666.67	m^3	80.0	3.00E+03	2.88E+03		11,229	USD 898,346
NaOH make-up tank	1.0	21.0	248.34	m^3	12.0	3.00E+03	2.88E+03		11,229	USD 134,752
Reacion tanks agitator	5.0	400.0	248.34	m^3	1.0	7.22E+00	2.23E-01	-9.326E-05	20,522	USD 20,522
NaOH dosage pump	1.4	27.2	41.39	m^3/h	2.0	1.13E+05	3.77E-01		89,036	USD 178,072
Feed tank agitator	5.0	400.0	1666.67	m^3	80.0	7.22E+00	2.23E-01	-9.326E-05	20,522	USD 1,641,733
Product pump	1.4	27.2	836.37	m^3/h	31.0	1.13E+05	3.77E-01		15553	USD 482,150
Filter, press, plate & frame, manual	4.0	18.0	5.132	m^2	1.0	3.71E+01	2.08E+01	-5.550E-01	58,282	USD 58,282
SUB-TOTAL										USD 4,964,336
Factor for civils, piping, instrumentation etc.	2.00			factor						USD 9,928,672

Figure C-1. CAPEX outline flowsheet 1.1/2

Item	size					a	b	c	Cost	Cost
	smallest	largest	used	used					R('000)	R('000)
Precipitation 1	Min	Max	Used			a	b	c	Cost/unit	USD 15,148,200
Reaction tanks	1.0	21.0	1808.94	m^3	87.0	3.00E+03	2.88E+03		11,229	USD 976,952
Reacion tanks agitator	5.0	400.0	1808.94	m^3	5.0	7.22E+00	2.23E-01	-9.326E-05	20,522	USD 102,608
Feed pump	1.4	27.2	833.33	m^3/h	31.0	1.13E+05	3.77E-01		15553	USD 482,150
Feed tank	1.0	21.0	1666.67	m^3	80.0	3.00E+03	2.88E+03		11,229	USD 898,346
NaOH make-up tank	1.0	21.0	248.34	m^3	12.0	3.00E+03	2.88E+03		11,229	USD 134,752
Reacion tanks agitator	5.0	400.0	248.34	m^3	1.0	7.22E+00	2.23E-01	-9.326E-05	20,522	USD 20,522
NaOH dosage pump	1.4	27.2	41.39	m^3/h	2.0	1.13E+05	3.77E-01		89,036	USD 178,072
Feed tank agitator	5.0	400.0	1666.67	m^3	80.0	7.22E+00	2.23E-01	-9.326E-05	20,522	USD 1,641,733
Product pump	1.4	27.2	844.17	m^3/h	32.0	1.13E+05	3.77E-01		15553	USD 497,703
Filter, press, plate & frame, manual	4.0	18.0	35.541	m^2	2.0	3.71E+01	2.08E+01	-5.550E-01	58,282	USD 116,563
SUB-TOTAL										USD 5,049,400
Factor for civils, piping, instrumentation etc.	2.00			factor						USD 10,098,800

Figure C-2. CAPEX outline flowsheet 1.3/4

Item	size					a	b	c	Cost	Cost
	smallest	largest	used	used					R('000)	R('000)
Precipitation 1	Min	Max	Used			a	b	c	Cost/unit	USD 14,893,008
Reaction tanks	1.0	21.0	1792.23	m^3	86.0	3.00E+03	2.88E+03		11,229	USD 965,722
Reacion tanks agitator	5.0	400.0	1792.23	m^3	5.0	7.22E+00	2.23E-01	-9.326E-05	20,522	USD 102,608
Feed pump	1.4	27.2	833.33	m^3/h	31.0	1.13E+05	3.77E-01		15553	USD 482,150
Feed tank	1.0	21.0	1666.67	m^3	80.0	3.00E+03	2.88E+03		11,229	USD 898,346
NaOH make-up tank	1.0	21.0	248.34	m^3	12.0	3.00E+03	2.88E+03		11,229	USD 134,752
Reacion tanks agitator	5.0	400.0	248.34	m^3	1.0	7.22E+00	2.23E-01	-9.326E-05	20,522	USD 20,522
NaOH dosage pump	1.4	27.2	41.39	m^3/h	2.0	1.13E+05	3.77E-01		89,036	USD 178,072
Feed tank agitator	5.0	400.0	1666.67	m^3	80.0	7.22E+00	2.23E-01	-9.326E-05	20,522	USD 1,641,733
Product pump	1.4	27.2	836.37	m^3/h	31.0	1.13E+05	3.77E-01		15553	USD 482,150
Filter, press, plate & frame, manual	4.0	18.0	5.132	m^2	1.0	3.71E+01	2.08E+01	-5.550E-01	58,282	USD 58,282
SUB-TOTAL										USD 4,964,336
Factor for civils, piping, instrumentation etc.	2.00			factor						USD 9,928,672
Precipitation 2	Min	Max	Used			a	b	c	Cost/unit	USD 18,942,256
Reaction tanks	1.0	21.0	2300.9	m^3	110.0	3.00E+03	2.88E+03		11,229	USD 1,235,226
Reaction tanks agitator	5.0	400.0	2300.9	m^3	110.0	7.22E+00	2.23E-01	-9.326E-05	20,522	USD 2,257,383
Feed tank	1.0	21.0	2091.2	m^3	100.0	3.00E+03	2.88E+03		11,229	USD 1,122,933
NaOH make-up tank	1.0	21.0	165.6	m^3	8.0	3.00E+03	2.88E+03		11,229	USD 89,835
Reaction tanks agitator	5.0	400.0	165.6		1.0	7.22E+00	2.23E-01	-9.326E-05	20,522	USD 20,522
NaOH dosage pump	1.4	27.2	27.6	m^3/h	2.0	1.13E+05	3.77E-01		89,036	USD 178,072
Feed tank agitator	5.0	400.0	2091.2	m^3	6.0	7.22E+00	2.23E-01	-9.326E-05	20,522	USD 123,130
Feed pump	1.4	27.2	1045.6	m^3/h	39.0	1.13E+05	3.77E-01		15553	USD 606,575
Product pump	1.4	27.2	1073.8	m^3/h	40.0	1.13E+05	3.77E-01		15553	USD 622,128
Filter, press, plate & frame, manual	4.0	18.0	2.25	m^2	1.0	3.71E+01	2.08E+01	-5.550E-01	58,282	USD 58,282
SUB-TOTAL										USD 6,314,085
Factor for civils, piping, instrumentation etc.	2.00			factor						USD 12,628,170

Figure C-3. CAPEX outline flowsheet 2.1/2

Item	size					a	b	c	Cost	Cost
	smallest	largest	used	used					R('000)	R('000)
Precipitation 1	Min	Max	Used			a	b	c	Cost/unit	USD 15,148,200
Reaction tanks	1.0	21.0	1808.94	m^3	87.0	3.00E+03	2.88E+03		11,229	USD 976,952
Reacion tanks agitator	5.0	400.0	1808.94	m^3	5.0	7.22E+00	2.23E-01	-9.326E-05	20,522	USD 102,608
Feed pump	1.4	27.2	833.33	m^3/h	31.0	1.13E+05	3.77E-01		15553	USD 482,150
Feed tank	1.0	21.0	1666.67	m^3	80.0	3.00E+03	2.88E+03		11,229	USD 898,346
NaOH make-up tank	1.0	21.0	248.34	m^3	12.0	3.00E+03	2.88E+03		11,229	USD 134,752
Reacion tanks agitator	5.0	400.0	248.34	m^3	1.0	7.22E+00	2.23E-01	-9.326E-05	20,522	USD 20,522
NaOH dosage pump	1.4	27.2	41.39	m^3/h	2.0	1.13E+05	3.77E-01		89,036	USD 178,072
Feed tank agitator	5.0	400.0	1666.67	m^3	80.0	7.22E+00	2.23E-01	-9.326E-05	20,522	USD 1,641,733
Product pump	1.4	27.2	844.17	m^3/h	32.0	1.13E+05	3.77E-01		15553	USD 497,703
Filter, press, plate & frame, manual	4.0	18.0	35.541	m^2	2.0	3.71E+01	2.08E+01	-5.550E-01	58,282	USD 116,563
SUB-TOTAL										USD 5,049,400
Factor for civils, piping, instrumentation etc.	2.00			factor						USD 10,098,800
Precipitation 2	Min	Max	Used			a	b	c	Cost/unit	USD 39,805,584
Reaction tanks	1.0	21.0	4982.0	m^3	238.0	3.00E+03	2.88E+03		11,229	USD 2,672,580
Reaction tanks agitator	5.0	400.0	4982.0	m^3	238.0	7.22E+00	2.23E-01	-9.326E-05	20,522	USD 4,884,157
Feed tank	1.0	21.0	4586.3	m^3	219.0	3.00E+03	2.88E+03		11,229	USD 2,459,223
NaOH make-up tank	1.0	21.0	165.6	m^3	8.0	3.00E+03	2.88E+03		11,229	USD 89,835
Reaction tanks agitator	5.0	400.0	165.6		1.0	7.22E+00	2.23E-01	-9.326E-05	20,522	USD 20,522
NaOH dosage pump	1.4	27.2	27.6	m^3/h	2.0	1.13E+05	3.77E-01		89,036	USD 178,072
Feed tank agitator	5.0	400.0	4586.3	m^3	12.0	7.22E+00	2.23E-01	-9.326E-05	20,522	USD 246,260
Feed pump	1.4	27.2	2293.2	m^3/h	85.0	1.13E+05	3.77E-01		15553	USD 1,322,023
Product pump	1.4	27.2	2324.9	m^3/h	86.0	1.13E+05	3.77E-01		15553	USD 1,337,576
Filter, press, plate & frame, manual	4.0	18.0	16.35	m^2	1.0	3.71E+01	2.08E+01	-5.550E-01	58,282	USD 58,282
SUB-TOTAL										USD 13,268,528
Factor for civils, piping, instrumentation etc.	2.00			factor						USD 26,537,056

Figure C-4. CAPEX outline flowsheet 2.3

Item	size					a	b	c	Unit Cost	Total Cost
	smallest	largest	used	used					R('000)	R('000)
Precipitation 1	Min	Max	Used			a	b	c	Cost/unit	USD 14,148,165
Reaction tanks	1.0	21.0	1808.94	m^3	87.0	3.00E+03	2.88E+03		11,229	USD 976,952
Reacion tanks agitator	5.0	400.0	1808.94	m^3	5.0	7.22E+00	2.23E-01	-9.326E-05	20,522	USD 102,608
Feed pump	1.4	27.2	833.33	m^3/h	31.0	1.13E+05	3.77E-01		15553	USD 482,150
Feed tank	1.0	21.0	1666.67	m^3	80.0	3.00E+03	2.88E+03		11,229	USD 898,346
NaOH make-up tank	1.0	21.0	248.3	m3	12.0	3.00E+03	2.88E+03		11,229	
Reacion tanks agitator	5.0	400.0	248.3	m3	1.0	7.22E+00	2.23E-01	-9.326E-05	20,522	
NaOH dosage pump	1.4	27.2	41.4	m3/h	2.0	1.13E+05	3.77E-01		89,036	
Feed tank agitator	5.0	400.0	1666.67	m^3	80.0	7.22E+00	2.23E-01	-9.326E-05	20,522	USD 1,641,733
Product pump	1.4	27.2	844.17	m^3/h	32.0	1.13E+05	3.77E-01		15553	USD 497,703
Filtrate tank					#DIV/0!					
Wash water tank					#DIV/0!					
Filter, press, plate & frame, manual	4.0	18.0	35.541	m^2	2.0	3.71E+01	2.08E+01	-5.550E-01	58,282	USD 116,563
SUB-TOTAL										USD 4,716,055
Factor for civils, piping, instrumentation etc.	2.00			factor						USD 9,432,110
Precipitation 2	Min	Max	Used			a	b	c	Cost/unit	USD 41,175,472
Reaction tanks	1.0	21.0	5085.6	m^3	243.0	3.00E+03	2.88E+03		11,229	USD 2,728,727
Reaction tanks agitator	5.0	400.0	5085.6	m^3	243.0	7.22E+00	2.23E-01	-9.326E-05	20,522	USD 4,986,765
Feed tank	1.0	21.0	4586.3	m^3	219.0	3.00E+03	2.88E+03		11,229	USD 2,459,223
NaOH make-up tank	1.0	21.0	455.6	m3	22.0	3.00E+03	2.88E+03		11,229	USD 247,045
Reacion tanks agitator	5.0	400.0	455.6	m3	2.0	7.22E+00	2.23E-01	-9.326E-05	20,522	USD 41,043
NaOH dosage pump	1.4	27.2	75.9	m3/h	3.0	1.13E+05	3.77E-01		89,036	USD 267,107
Feed tank agitator	5.0	400.0	4586.3	m^3	12.0	7.22E+00	2.23E-01	-9.326E-05	20,522	USD 246,260
Feed pump	1.4	27.2	2293.2	m^3/h	85.0	1.13E+05	3.77E-01		15553	USD 1,322,023
Product pump	1.4	27.2	2373.3	m^3/h	88.0	1.13E+05	3.77E-01		15553	USD 1,368,682
Filter, press, plate & frame, manual	4.0	18.0	16.35	m^2	1.0	3.71E+01	2.08E+01	-5.550E-01	58,282	USD 58,282
SUB-TOTAL										USD 13,725,157
Factor for civils, piping, instrumentation etc.	2.00			factor						USD 27,450,315
Precipitation 3	Min	Max	Used			a	b	c	Cost/unit	USD 38,676,154
Reaction tanks	1.0	21.0	4321.2	m^3	206.0	3.00E+03	2.88E+03		11,229	USD 2,313,241
Reaction tanks agitator	5.0	400.0	4321.2	m^3	206.0	7.22E+00	2.23E-01	-9.326E-05	20,522	USD 4,227,463
Feed tank	1.0	21.0	3899.8	m^3	186.0	3.00E+03	2.88E+03		11,229	USD 2,088,655
NaOH make-up tank	1.0	21.0	387.4	m3	19.0	3.00E+03	2.88E+03		11,229	
Reacion tanks agitator	5.0	400.0	387.4	m3	1.0	7.22E+00	2.23E-01	-9.326E-05	20,522	
NaOH dosage pump	1.4	27.2	64.6	m3/h	3.0	1.13E+05	3.77E-01		89,036	
Feed tank agitator	5.0	400.0	3899.8	m^3	10.0	7.22E+00	2.23E-01	-9.326E-05	20,522	USD 205,217
Feed pump	1.4	27.2	2014.5	m^3/h	75.0	1.13E+05	3.77E-01		15553	USD 1,166,491
Product pump	1.4	27.2	2016.6	m^3/h	75.0	1.13E+05	3.77E-01		15553	USD 1,166,491
Filter, press, plate & frame, manual	4.0	18.0	8.27	m^2	1.0	3.71E+01	2.08E+01	-5.550E-01	58,282	USD 58,282
SUB-TOTAL										USD 11,225,840
Factor for civils, piping, instrumentation etc.	2.00			factor						USD 27,450,315

Figure C-5. CAPEX outline flowsheet 2.4

Item	size					a	b	c	Cost	Cost
	smallest	largest	used	used					R('000)	R('000)
Precipitation 1	Min	Max	Used			a	b	c	Cost/unit	USD 19,879,773
Reaction tanks	1.0	21.0	1792.68	m^3	86.0	3.00E+03	2.88E+03		11,229	USD 965,722
Reacion tanks agitator	5.0	400.0	1792.68	m^3	86.0	7.22E+00	2.23E-01	-9.326E-05	20,522	USD 1,764,863
Feed pump	1.4	27.2	833.33	m^3/h	31.0	1.13E+05	3.77E-01		15553	USD 482,150
Feed tank	1.0	21.0	1666.67	m^3	80.0	3.00E+03	2.88E+03		11,229	USD 898,346
NaOH make-up tank	1.0	21.0	248.3	m3	12.0	3.00E+03	2.88E+03		11,229	USD 134,752
Reacion tanks agitator	5.0	400.0	248.3	m3	1.0	7.22E+00	2.23E-01	-9.326E-05	20,522	USD 20,522
NaOH dosage pump	1.4	27.2	41.4	m3/h	2.0	1.13E+05	3.77E-01		89,036	USD 178,072
Feed tank agitator	5.0	400.0	1666.67	m^3	80.0	7.22E+00	2.23E-01	-9.326E-05	20,522	USD 1,641,733
Product pump	1.4	27.2	836.58	m^3/h	31.0	1.13E+05	3.77E-01		15553	USD 482,150
Filter, press, plate & frame, manual	4.0	18.0	5.955	m^2	1.0	3.71E+01	2.08E+01	-5.550E-01	58,282	USD 58,282
SUB-TOTAL										USD 6,626,591
Factor for civils, piping, instrumentation etc.	2.00			factor						USD 13,253,182
Precipitation 2	Min	Max	Used			a	b	c	Cost/unit	USD 25,259,726
Reaction tanks	1.0	21.0	2372.5	m^3	113.0	3.00E+03	2.88E+03		11,229	USD 1,268,914
Reaction tanks agitator	5.0	400.0	2372.5	m^3	113.0	7.22E+00	2.23E-01	-9.326E-05	20,522	USD 2,318,948
Feed tank	1.0	21.0	2158.7	m^3	103.0	3.00E+03	2.88E+03		11,229	USD 1,156,621
NaOH make-up tank	1.0	21.0	165.6	m3	8.0	3.00E+03	2.88E+03		11,229	USD 89,835
Reacion tanks agitator	5.0	400.0	165.6	m3	1.0	7.22E+00	2.23E-01	-9.326E-05	20,522	USD 20,522
NaOH dosage pump	1.4	27.2	27.6	m3/h	2.0	1.13E+05	3.77E-01		89,036	USD 178,072
Feed tank agitator	5.0	400.0	2158.7	m^3	103.0	7.22E+00	2.23E-01	-9.326E-05	20,522	USD 2,113,732
Feed pump	1.4	27.2	1079.4	m^3/h	40.0	1.13E+05	3.77E-01		15553	USD 622,128
Product pump	1.4	27.2	1107.2	m^3/h	41.0	1.13E+05	3.77E-01		15553	USD 637,682
Filter, press, plate & frame, manual	4.0	18.0	0.81	m^2	1.0	3.71E+01	2.08E+01	-5.550E-01	13,456	USD 13,456
SUB-TOTAL										USD 8,419,909
Factor for civils, piping, instrumentation etc.	2.00			factor						USD 16,839,818
Calcination	Min	Max	Used			a	b	c	Cost/unit	USD 3,343,000
Coal fired rotary kiln	0.12	0.5	0.83	t/h	1.7	4.43E+02	4.46E+03	-7.04E+00	671,979	USD 1,110,025
pump precip1 prod	1.40	27.2	0.34	m3/h	1.0	6.81E+00	9.28E-02	6.82E-06	1,747	USD 1,747
pump precip 2 prod	3.60	27.2	36.20	m3/h	1.0	6.81E+00	9.28E-02	6.82E-06	2,561	USD 2,561
										USD 1,114,333
Factor for civils, piping, instrumentation etc.	2.00			factor						USD 2,228,666.37

Figure C-6. CAPEX outline flowsheet 3.1

Item	size					a	b	c	Cost	Cost
	smallest	largest	used	used					R('000)	R('000)
Precipitation 1	Min	Max	Used			a	b	c	Cost/unit	USD 20,371,375
Reaction tanks	1.0	21.0	1812.26	m^3	87.0	3.00E+03	2.88E+03		11,229	USD 976,952
Reacion tanks agitator	5.0	400.0	1812.26	m^3	87.0	7.22E+00	2.23E-01	-9.326E-05	20,522	USD 1,785,385
Feed pump	1.4	27.2	833.33	m^3/h	31.0	1.13E+05	3.77E-01		15553	USD 482,150
Feed tank	1.0	21.0	1666.67	m^3	80.0	3.00E+03	2.88E+03		11,229	USD 898,346
NaOH make-up tank	1.0	21.0	248.3	m3	12.0	3.00E+03	2.88E+03		11,229	USD 134,752
Reacion tanks agitator	5.0	400.0	248.3	m3	1.0	7.22E+00	2.23E-01	-9.326E-05	20,522	USD 20,522
NaOH dosage pump	1.4	27.2	41.4	m3/h	2.0	1.13E+05	3.77E-01		89,036	USD 178,072
Feed tank agitator	5.0	400.0	1666.67	m^3	80.0	7.22E+00	2.23E-01	-9.326E-05	20,522	USD 1,641,733
Product pump	1.4	27.2	845.72	m^3/h	32.0	1.13E+05	3.77E-01		15553	USD 497,703
Filter, press, plate & frame, manual	4.0	18.0	41.590	m^2	3.0	3.71E+01	2.08E+01	-5.550E-01	58,282	USD 174,845
SUB-TOTAL										USD 6,790,458
Factor for civils, piping, instrumentation etc.	2.00			factor						USD 13,580,917
Precipitation 2	Min	Max	Used			a	b	c	Cost/unit	USD 57,988,549
Reaction tanks	1.0	21.0	5508.1	m^3	263.0	3.00E+03	2.88E+03		11,229	USD 2,953,313
Reaction tanks agitator	5.0	400.0	5508.1	m^3	263.0	7.22E+00	2.23E-01	-9.326E-05	20,522	USD 5,397,199
Feed tank	1.0	21.0	5082.6	m^3	243.0	3.00E+03	2.88E+03		11,229	USD 2,728,727
NaOH make-up tank	1.0	21.0	165.6	m3	8.0	3.00E+03	2.88E+03		11,229	USD 89,835
Reacion tanks agitator	5.0	400.0	165.6	m3	1.0	7.22E+00	2.23E-01	-9.326E-05	20,522	USD 20,522
NaOH dosage pump	1.4	27.2	27.6	m3/h	2.0	1.13E+05	3.77E-01		89,036	USD 178,072
Feed tank agitator	5.0	400.0	5082.6	m^3	243.0	7.22E+00	2.23E-01	-9.326E-05	20,522	USD 4,986,765
Feed pump	1.4	27.2	2541.3	m^3/h	94.0	1.13E+05	3.77E-01		15553	USD 1,462,002
Product pump	1.4	27.2	2570.4	m^3/h	95.0	1.13E+05	3.77E-01		15553	USD 1,477,555
Filter, press, plate & frame, manual	4.0	18.0	5.95	m^2	1.0	3.71E+01	2.08E+01	-5.550E-01	35,528	USD 35,528
SUB-TOTAL										USD 19,329,516
Factor for civils, piping, instrumentation etc.	2.00			factor						USD 38,659,033
Calcination	Min	Max	Used			a	b	c	Cost/unit	USD 24,623,570
Coal fired rotary kiln	0.12	0.5	6.10	t/h	12.2	4.43E+02	4.46E+03	-7.04E+00	671,979	USD 8,203,548
pump precip1 prod	1.40	27.2	0.34	m3/h	1.0	6.81E+00	9.28E-02	6.82E-06	1,747	USD 1,747
pump precip 2 prod	3.60	27.2	36.20	m3/h	1.0	6.81E+00	9.28E-02	6.82E-06	2,561	USD 2,561
										USD 8,207,857
Factor for civils, piping, instrumentation etc.	2.00			factor						USD 16,415,713.30

Figure C-7. CAPEX outline flowsheet 3.2